

Assessment of CMIP6 Sea Ice Concentration and Thickness with Observation

THOMAS AMO KYEIMIAH (STUDENT)
HOUSSEYNI SANKARE (SUPERVISOR)

CONTENTS

CONTENTS.....	1
TABLES	2
FIGURES	2
1 INTRODUCTION	4
1.1 BACKGROUND.....	4
1.2 OBJECTIVES	5
2 DATA	6
2.1 CMIP6 MODEL DATA	6
2.2 OBSERVATIONAL DATA	7
3 METHODOLOGY	8
3.1 DATA PREPROCESSING.....	8
3.2 STATISTICAL EVALUATION METRICS	8
3.3 TEMPORAL TREND ANALYSIS FOR SELECTED REGIONS.....	9
4 RESULTS	11
4.1 SEA ICE CONCENTRATION	11
4.1.1 SPATIAL DISTRIBUTION	11
4.1.2 TEMPORAL TRENDS	14
4.2 SEA ICE THICKNESS	19
4.2.1 SPATIAL DISTRIBUTION.....	19
4.2.2 TEMPORAL TRENDS	22
5 DISCUSSION	27
6 CONCLUSION.....	28
7 DATA AVAILABILITY	29
8 BIBLIOGRAPHY	29
9 APPENDIX.....	31
9.1 SIC.....	31
9.2 SIT	44

TABLES

Table 1: CMIP6 Models Used for SIC and SIT Evaluations.....	6
Table 2: Observational Data Used for SIC and SIT Evaluations.....	7
Table 3: Selected Sub-regions in the Ocean around Canada	10

FIGURES

Figure 1: Map showing the eight sub-regions in the ocean around Canada used for the assessment of CMIP6 SIC and SIT. The sub-regions are identified by different colors and abbreviations of each region's name	9
Figure 2: Spatial distribution of mean sea ice concentration (SIC) and mean bias of the median (50th percentile) from 1982-2014. The top row shows the mean SIC from the HadISST dataset (left) and OSTIA dataset (right). The bottom row displays the mean bias of the median SIC from CMIP6 models relative to HadISST (left) and OSTIA (right).	11
Figure 3: Spatial distribution of mean sea ice concentration (SIC) and percentage bias of the median (50th percentile) from 1982-2014. The top row shows the mean SIC from the HadISST dataset (left) and OSTIA dataset (right). The bottom row displays the mean bias of the median SIC from CMIP6 models relative to HadISST (left) and OSTIA (right).	12
Figure 4: Spatial distribution of MAM SIC and MAM bias of the median (50th percentile) from 1982-2014. The top row shows the MAM SIC from the HadISST dataset (left) and OSTIA dataset (right). The bottom row displays the MAM bias of the median SIC from CMIP6 models relative to HadISST (left) and OSTIA (right).	13
Figure 5: Spatial distribution of DJF SIC and DJF bias of the median (50th percentile) from 1982-2014. The top row shows the DJF SIC from the HadISST dataset (left) and OSTIA dataset (right). The bottom row displays the MAM bias of the median SIC from CMIP6 models relative to HadISST (left) and OSTIA (right).	14
Figure 6: Modeled percentiles and observed temporal trends of yearly SIC in the Beaufort Sea from 1982 to 2014.....	15
Figure 7: Modeled percentiles and observed temporal trends of yearly SIC in the Gulf of St. Lawrence from 1982 to 2014.	15
Figure 8: Modeled percentiles and observed temporal trends of yearly SIC in the Hudson Bay from 1982 to 2014.....	16
Figure 9: Modeled percentiles and observed temporal trends of yearly SIC in the Northern Labrador Shelf from 1982 to 2014.....	16
Figure 10: Modeled percentiles and observed temporal trends of yearly SIC in the Northern Newfoundland Shelf from 1982 to 2014.	17

Figure 11: Modeled percentiles and observed temporal trends of yearly SIC in the Southern Newfoundland Shelf from 1982 to 2014.....	17
Figure 12: Modeled percentiles and observed temporal trends of yearly SIC in the Arctic Ocean Shelf from 1982 to 2014.....	18
Figure 13: Modeled percentiles and observed temporal trends of yearly SIC in the Baffin Bay from 1982 to 2014.....	18
Figure 14: Spatial distribution of mean sea ice thickness (SIT) and mean bias of the median (50th percentile) from 1982-2014. The top row shows the mean SIT from the PIOMAS dataset (left) and C3S dataset (right). The bottom row displays the mean bias of the median SIT from CMIP6 models relative to PIOMAS (left) and C3S (right)......	19
Figure 15: Spatial distribution of mean sea ice thickness (SIT) and percentage bias of the median (50th percentile) from 1982-2014. The top row shows the mean SIT from the PIOMAS dataset (left) and C3S dataset (right). The bottom row displays the percentage bias of the median SIT from CMIP6 models relative to PIOMAS (left) and C3S (right)......	20
Figure 16: Spatial distribution of MAM sea ice thickness (SIT) and MAM bias of the median (50th percentile) from 1982-2014. The top row shows the MAM SIT from the PIOMAS dataset (left) and C3S dataset (right). The bottom row displays the MAM bias of the median SIT from CMIP6 models relative to PIOMAS (left) and C3S (right)......	21
Figure 17: Spatial distribution of DJF sea ice thickness (SIT) and DJF bias of the median (50th percentile) from 1982-2014. The top row shows the DJF SIT from the PIOMAS dataset (left) and C3S dataset (right). The bottom row displays the DJF bias of the median SIT from CMIP6 models relative to PIOMAS (left) and C3S (right)......	22
Figure 18: Modeled percentiles and observed temporal trends of yearly SIT in the Beaufort Sea from 1982 to 2014	23
Figure 19: Modeled percentiles and observed temporal trends of yearly SI in the Gulf of St. Lawrence from 1982 to 2014.	24
Figure 20: Modeled percentiles and observed temporal trends of yearly SIT in Hudson Bay from 1982 to 2014.....	24
Figure 21: Modeled percentiles and observed temporal trends of yearly SIT in the Northern Labrador Shelf from 1982 to 2014.	25
Figure 22: Modeled percentiles and observed temporal trends of yearly SIT in the Northern Newfoundland Shelf from 1982 to 2014.....	25
Figure 23: Modeled percentiles and observed temporal trends of yearly SIT in the Arctic Ocean Shelf from 1982 to 2014.....	26
Figure 24: Modeled percentiles and observed temporal trends of yearly SIT in the Arctic Ocean Shelf from 1982 to 2014.....	26
Figure 25: Modeled percentiles and observed temporal trends of yearly SIT in the Southern Labrador Shelf from 1982 to 2014	27

1 INTRODUCTION

1.1 BACKGROUND

The Arctic region is crucial to the global climate system, acting as a significant regulator of Earth's energy balance. Sea ice is a critical component and most sensitive indicator of the Earth's climate system, particularly in polar regions such as the Arctic. It is the most sensitive climate change indicator of the Arctic (Döscher, Vihma, & Maksimovich, 2014) and plays a significant role in regulating the global climate system by influencing the albedo effect, moderating ocean-atmosphere heat exchange, and impacting global ocean circulation patterns (Vihma, 2014; Bhatt, et al., 2014). In Canada, sea ice dynamics are especially important due to the extensive ice-covered areas in the Arctic Archipelago, Hudson Bay, etc., which have significant implications for local ecosystems, indigenous communities, shipping routes, and resource extraction activities (Barber, et al., 2012). Understanding sea ice concentration and thickness in this region is essential for predicting future climate changes and for developing effective adaptation and mitigation strategies.

In the Canadian Arctic, sea ice concentration (SIC) and sea ice thickness (SIT) are critical parameters for assessing the state of sea ice. Sea ice concentration refers to the proportion of an area covered by ice, while sea ice thickness measures the vertical extent of the ice layer. Both parameters are influenced by various factors, including atmospheric conditions, ocean currents, and heat fluxes. Over recent decades, the Arctic has experienced dramatic changes, including a marked decline in sea ice concentration, extent and thickness, primarily driven by anthropogenic climate change (Bhatt, et al., 2014; Post, et al., 2013). These changes have led to a growing need for accurate predictions of future sea ice conditions to inform policy and adaptation strategies. Accurate simulations of SIC and SIT are essential for understanding sea ice dynamics, forecasting future changes, and assessing the impacts of climate change on Arctic environments

The Coupled Model Intercomparison Project Phase 6 (CMIP6) represents the latest generation of global climate models (GCMs) used to simulate the Earth's climate system and project future climate scenarios. Climate models participating in CMIP6 have shown marked improvement in simulating sea-ice cover compared to prior phases (Henke, et al., 2023). The CMIP6 models include significant advancements in simulating various components of the climate system, including sea ice. These advancements involve improved representations of sea ice physics, including both dynamics and thermodynamics, compared to their predecessors. However, the accuracy of these models in replicating observed sea ice conditions, particularly over regions like Canada, remains a critical area of research. This necessitates a detailed assessment of CMIP6 models to understand their strengths and weaknesses in simulating sea ice concentration and thickness in this critical region.

1.2 OBJECTIVES

The primary objective is to evaluate the performance of CMIP6 models in simulating sea ice concentration and thickness specifically over Canadian waters. This assessment aims to:

- Evaluate the Performance of CMIP6 Models:
 - Assess the accuracy and reliability of SIC and SIT outputs from CMIP6 models by comparing them with observational datasets for Canadian waters.
- Quantify Model Biases:
 - Analyze discrepancies or biases between CMIP6 model outputs and observational dataset.
- Improve Model Understanding:
 - Identify and provide insights into model deficiencies in certain regions.
- Support Decision-Making:
 - Provide valuable information and data available for ClimateData.ca.

Observational datasets offer temporal and spatial data on sea ice conditions, which are crucial for evaluating the performance of climate models. Thorough the assessment of CMIP6 SIC and SIT data against observations helps to quantify biases. By achieving these objectives, the report seeks to contribute to a more accurate understanding of sea ice dynamics in the Canadian Arctic, enhance the reliability of climate models, and support better-informed policy and decision-making processes related to Arctic environments.

2 DATA

To evaluate the performance of CMIP6 over Canadian waters, a comprehensive set of observational datasets and model outputs were utilized. This enables a detailed comparison of model simulations against observations, offering insights into the models' accuracy and reliability.

2.1 CMIP6 MODEL DATA

We used 20 CMIP6 models for the evaluation of SIC and 16 CMIP6 models for the evaluation of SIT. These models were selected based on four common emission scenarios: SSP1-2.6, SSP2-4.5, SSP3-7.0, and SSP5-8.5. They come from various climate modeling centers and feature different levels of complexity in their sea ice components, providing a comprehensive assessment of model performance. Each model offers monthly mean SIC and SIT data for historical periods and future projections, gridded to a common 1×1 degree resolution (see Table 1 for summary).

Table 1: CMIP6 Models Used for SIC and SIT Evaluations

CMIP6 Models	Sea Ice Concentration	Sea Ice Thickness
AWI-CM-1-1-MR		✓
BCC-CM2-MR	✓	
CAMS-CSM1-0	✓	
CESM2-WACCM	✓	✓
CESM2	✓	
CMCC-CM2-SR5	✓	✓
CMCC-ESM2	✓	✓
CanESM5	✓	✓
EC-Earth3-Veg-LR	✓	✓
EC-Earth3-Veg	✓	✓
EC-Earth3	✓	✓
FGOALS-f3-L	✓	
FGOALS-g3	✓	
IPSL-CM6A-LR	✓	✓
KACE-1-0-G		✓
MIROC6	✓	✓
MPI-ESM1-2-HR	✓	✓
MPI-ESM1-2-LR	✓	✓
MRI-ESM2-0	✓	✓
NorESM2-LM	✓	✓
NorESM2-MM	✓	✓
TaiESM1	✓	✓
Total	20	16

2.2 OBSERVATIONAL DATA

Table 2: Observational Data Used for SIC and SIT Evaluations

Variable	Name	Years of Record	Timestep	Spatial Resolution
Sea Ice Concentration	HadISST	1870-01 to 2024-03	Monthly	1° x 1°
	OSTIA	1981-10 to 2022-05	Daily	0.05° x 0.05°
Sea Ice Thickness	PIOMAS	1979-01 to 2023-01	Monthly	22km x 22km
	C3S	2002-10 to 202-04	Monthly	25km x 25km

- Sea Ice Concentration (SIC):
 - Hadley Centre Sea Ice and Sea Surface Temperature dataset (HadISST): We utilized the monthly HadISST dataset for sea ice concentration analysis. HadISST offers the longest continuous record of gridded sea ice data, covering the period from 1870 to the present at monthly intervals. The dataset provides a 1° x 1° spatially infilled grid, making it suitable for consistent analysis of sea surface temperatures (SST) and as boundary conditions for climate models. Version 1.1 of HadISST was employed in this study, which integrates a variety of data sources including historical ice charts, passive microwave satellite retrievals, and operational ice analyses from the National Centers for Environmental Prediction (NCEP) (Rayner, et al., 2003). The blending of these sources allows for a comprehensive and spatially complete dataset. This dataset is valuable for climate model evaluation due to its long temporal coverage and integration of multiple data sources (see Table 2 for summary).
 - Operational Sea Surface Temperature and Sea Ice Analysis (OSTIA): We also employed the daily OSTIA dataset, specifically the reprocessed global sea ice product (Good, et al., 2020). OSTIA provides daily, gap-free maps of foundation sea ice concentration at a high horizontal grid resolution of 0.05° x 0.05°, covering the period from 30 September 1981 to 30 May 2022. This dataset is derived from both in-situ and satellite observations, offering a detailed and precise representation of sea ice area fractions. OSTIA's fine spatial resolution is advantageous for capturing detailed sea ice conditions in complex regions such as the Canadian Arctic Archipelago (See Table 2 for summary).
- Sea Ice Thickness (SIT):
 - Pan-Arctic Ice Ocean Modeling and Assimilation System (PIOMAS): We use the monthly PIOMAS sea ice thickness, developed at the Applied Physics Laboratory and the Polar Science Center at the University of Washington (Zhang & Rothrock, 2003). PIOMAS has been extensively

validated through comparisons with observations from US-Navy submarines, oceanographic moorings, and satellites. The dataset spans from 1979 to the present and is frequently used to estimate Arctic Sea ice volume and thickness with a spatial resolution of 22×22 km (Schweiger, et al., 2011) (see Table 2 for summary).

- Copernicus Climate Change Service (C3S) Sea Ice Thickness Data: We also used the Arctic Sea ice Level 3 dataset, which provides monthly sea ice thickness data derived from reprocessed radar altimeter satellite observations (Envisat and CryoSat). This dataset covers the freezing season from October to April, spanning from September 30, 2002, to March 31, 2020, with a spatial resolution of 25×25 km (see Table 2 for summary).

3 METHODOLOGY

3.1 DATA PREPROCESSING

- Regridding and Interpolation: To ensure consistency across datasets, all observed observational data were regridded to the spatial resolution of the model's output grid. This step minimizes discrepancies due to differing grid resolutions. Bilinear interpolation was used for both SIC and SIT data to maintain the physical integrity of the ice, particularly in regions with sharp gradients or complex coastlines.
- Temporal Aggregation: We selected a common period based on the historical runs of the models HadISST, OSTIA, and PIOMAS from January 1982 to December 2014 while C3S was selected for the period from January 2003 to December 2014 due to the availability of data. The performance of the CMIP6 models was evaluated using a percentile-based approach, focusing on the 50th (median), 10th, and 90th percentiles of SIC and SIT from the model outputs. These percentiles provide insights into the distribution of sea ice conditions simulated by the models, capturing low, median, and high sea ice states. The 20 models for SIC were analyzed for their 50th, 10th, and 90th percentiles, similarly the 16 models for SIT were analyzed using the same approach. Monthly mean values of SIC and SIT were computed for both observed and model percentiles. These values were then aggregated into overall mean and seasonal means (e.g., DJF - December, January, February) to facilitate detailed comparisons across different seasons.

3.2 STATISTICAL EVALUATION METRICS

- Bias Calculation: The bias for each percentile was calculated as the difference between the model percentile value and the observed mean value:

$$Bias_P = Model_P - Observed$$

where P represents the specific percentile (10th, 50th, or 90th). This calculation was performed for both the overall mean and for each season (DJF, SON, etc.) to assess model performance under different conditions.

- Percentage Bias Calculation: The percentage bias was computed for each percentile to provide a normalized measure of model performance, indicating the relative deviation of model outputs from the observed mean:

$$\%Bias_P = \frac{Bias_P}{Observed} \times 100$$

This calculation was performed to provide a comprehensive view of model performance.

3.3 TEMPORAL TREND ANALYSIS FOR SELECTED REGIONS

To further assess the model's robustness, we evaluated the temporal trends of SIC and SIT over Canadian waters. Eight sub-regions within the ocean around Canada were selected. These regions represent different oceanic and sea ice environments, providing a comprehensive overview of the models' performance across diverse conditions. These sub-regions are listed in Table 3 and visually in Figure 1.

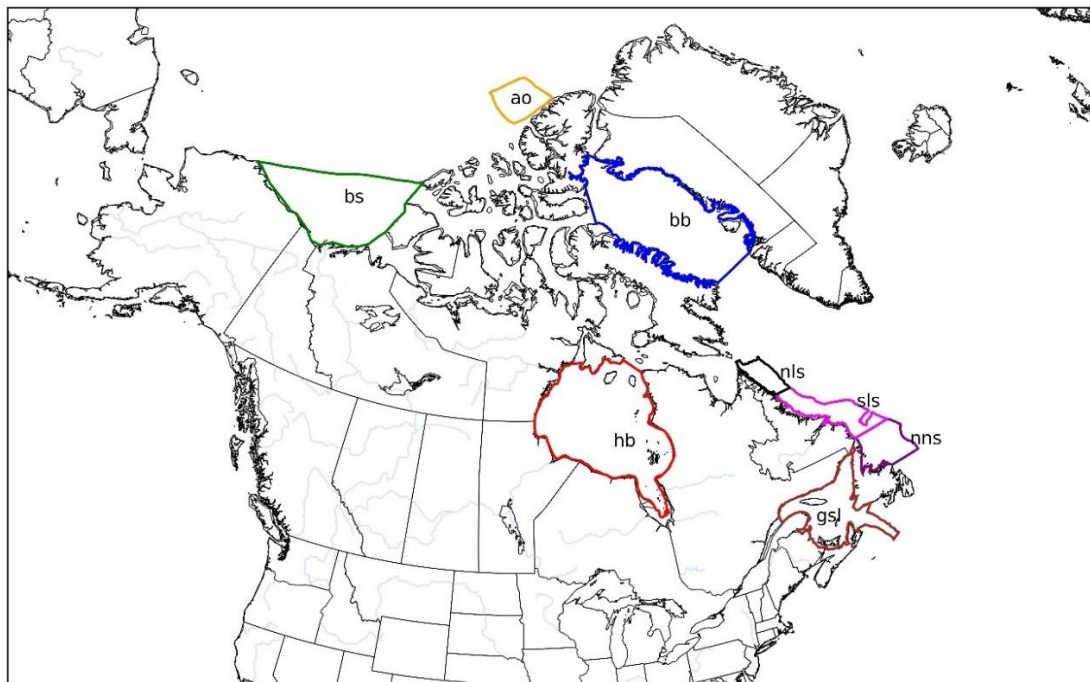


Figure 1: Map showing the eight sub-regions in the ocean around Canada used for the assessment of CMIP6 SIC and SIT. The sub-regions are identified by different colors and abbreviations of each region's name

For each sub-region, temporal trends in SIC and SIT were analyzed using the CMIP6 model percentiles and the mean observed data. The analysis focused on annual trends to capture the variability in model performance throughout the years. The temporal trends from the models were compared to the observed trends in each of the eight regions to evaluate the models' performance in capturing observed changes. The trends were computed for the historical period.

Table 3: Selected Sub-regions in the Ocean around Canada

Abbr.	Sub-region	Latitude	Longitude
gsl	Gulf of St. Lawrence	44.47 - 51.78	-67.21 - -56.19
nns	North Newfoundland Shelf	49.24 - 52.25	-56.73 - -50.10
sls	South Labrador Shelf	52.24 - 57.66	-61.70 - -51.15
nls	North Labrador Shelf	57.66 - 61.00	-64.50 - -59.50
hb	Hudson Bay	51.90 - 63.96	-94.69 - -76.66
bb	Baffin Bay	66.64 - 78.58	-82.19 - -50.13
bs	Beaufort Sea	69.09 - 76.20	-156.63 - -122.79
ao	Arctic Ocean	81.59 - 84.91	-111.95 - -79.78

4 RESULTS

4.1 SEA ICE CONCENTRATION

4.1.1 SPATIAL DISTRIBUTION

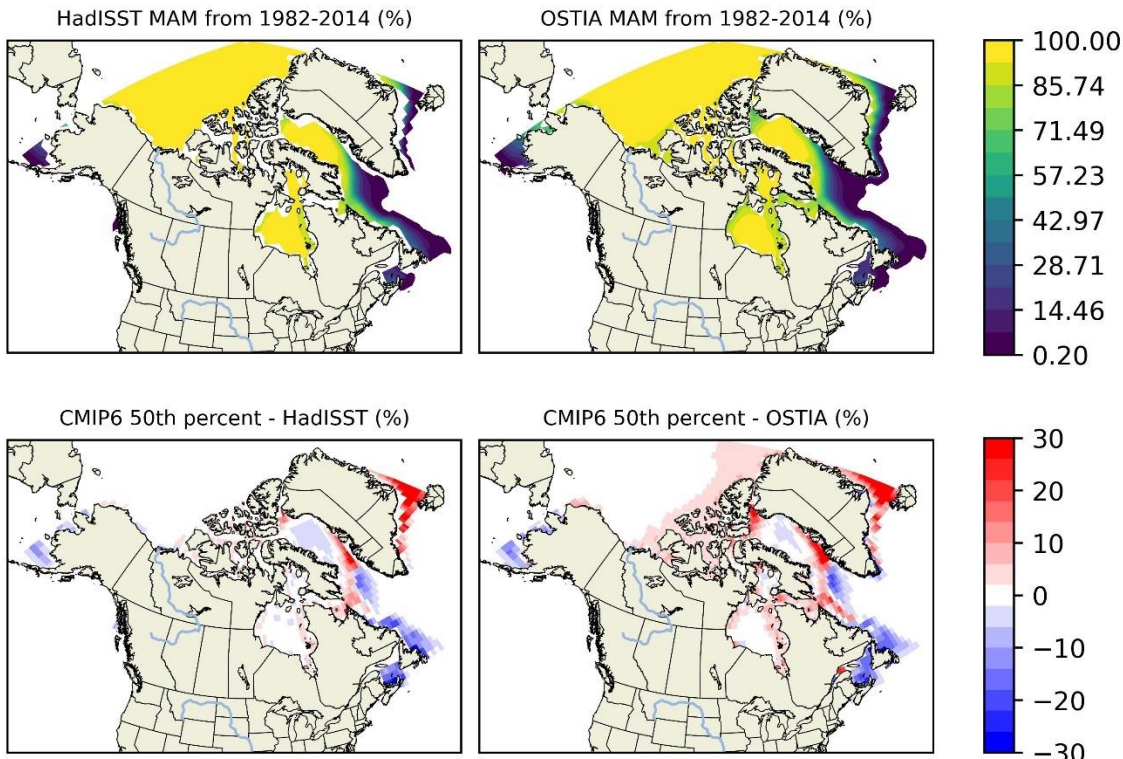


Figure 2: Spatial distribution of mean sea ice concentration (SIC) and mean bias of the median (50th percentile) from 1982-2014. The top row shows the mean SIC from the HadISST dataset (left) and OSTIA dataset (right). The bottom row displays the mean bias of the median SIC from CMIP6 models relative to HadISST (left) and OSTIA (right).

The analysis of SIC focused on the median (50th percentile) values to evaluate the models' ability to capture the central tendency of sea ice concentrations. The spatial distribution of the mean bias of the median SIC (Figure 2) indicated that most CMIP6 models tended to underestimate SIC in regions such as Hudson Bay, Beaufort Bay, and the Gulf of St. Lawrence, while overestimating it in the Canadian Arctic Archipelago, the northern part of Baffin Bay, and the western and southern parts of Greenland. The Arctic Ocean generally exhibited neutral (no) bias, despite a few small biases. HadISST generally showed smaller biases in regions with more stable ice, like the Arctic Ocean. In contrast, OSTIA's high-resolution data highlighted more significant overestimations in regions such as the southern part of Greenland, where persistent positive biases were prominent.

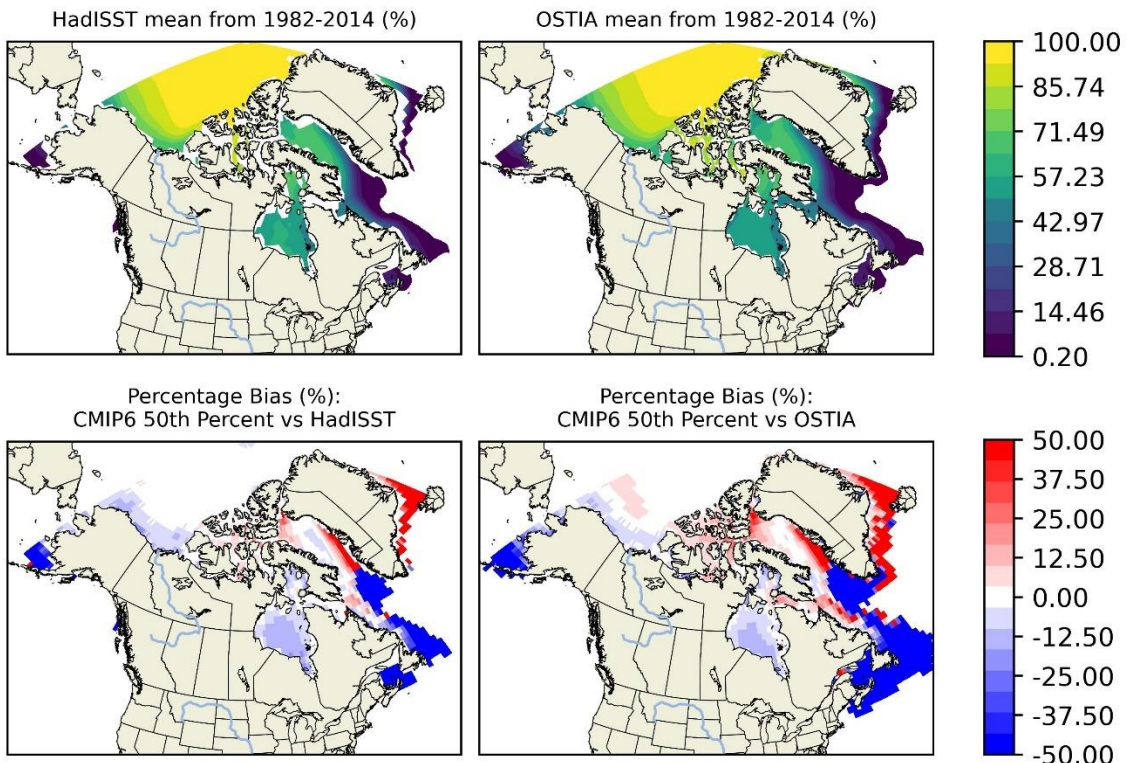


Figure 3: Spatial distribution of mean sea ice concentration (SIC) and percentage bias of the median (50th percentile) from 1982-2014. The top row shows the mean SIC from the HadISST dataset (left) and OSTIA dataset (right). The bottom row displays the mean bias of the median SIC from CMIP6 models relative to HadISST (left) and OSTIA (right).

The percentage bias of the median SIC (Figure 3) further emphasized the discrepancies between model outputs and observations. In regions with lower mean ice concentrations, such as Hudson Bay and the St. Lawrence Sea, and over the Labrador and Newfoundland shelves, the models showed higher negative percentage biases, ranging from -50% to -20%, particularly when compared to OSTIA. This suggests that the models struggle more with accurately representing thinner, more variable ice, where high-resolution data like OSTIA is particularly useful in identifying model weaknesses.

Despite these biases and discrepancies, the models generally performed well seasonally when compared to both datasets, capturing the broad patterns of SIC across different regions. Seasonal biases for the median SIC (Figure 4 - Figure 5), specifically for DJF (December, January, February) and MAM (March, April, May), revealed that biases were generally larger during the winter (DJF) than during the spring melt season (MAM). For instance, in MAM (Figure 4), the model slightly overestimated SIC across most regions when compared to OSTIA, while in DJF (Figure 5), the overestimations increased, particularly in eastern part of the arctic ocean, with the Canadian archipelago and southern

part of Greenland highlighted by OSTIA. This seasonal discrepancy suggests that while models capture the transitional periods relatively well, they face challenges during winter season. Hudson Bay, the Gulf of St. Lawrence, and the shelves of Newfoundland and Labrador experience negative biases, showing model underestimation in these regions.

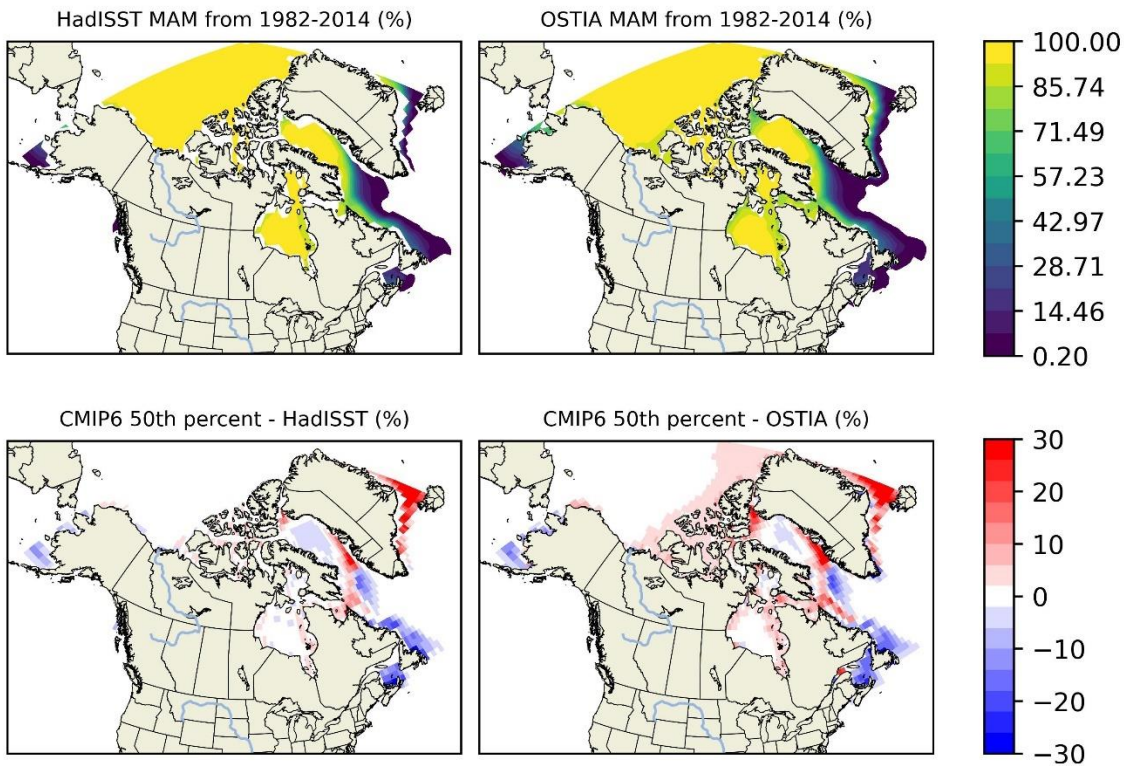


Figure 4: Spatial distribution of MAM SIC and MAM bias of the median (50th percentile) from 1982-2014. The top row shows the MAM SIC from the HadISST dataset (left) and OSTIA dataset (right). The bottom row displays the MAM bias of the median SIC from CMIP6 models relative to HadISST (left) and OSTIA (right).

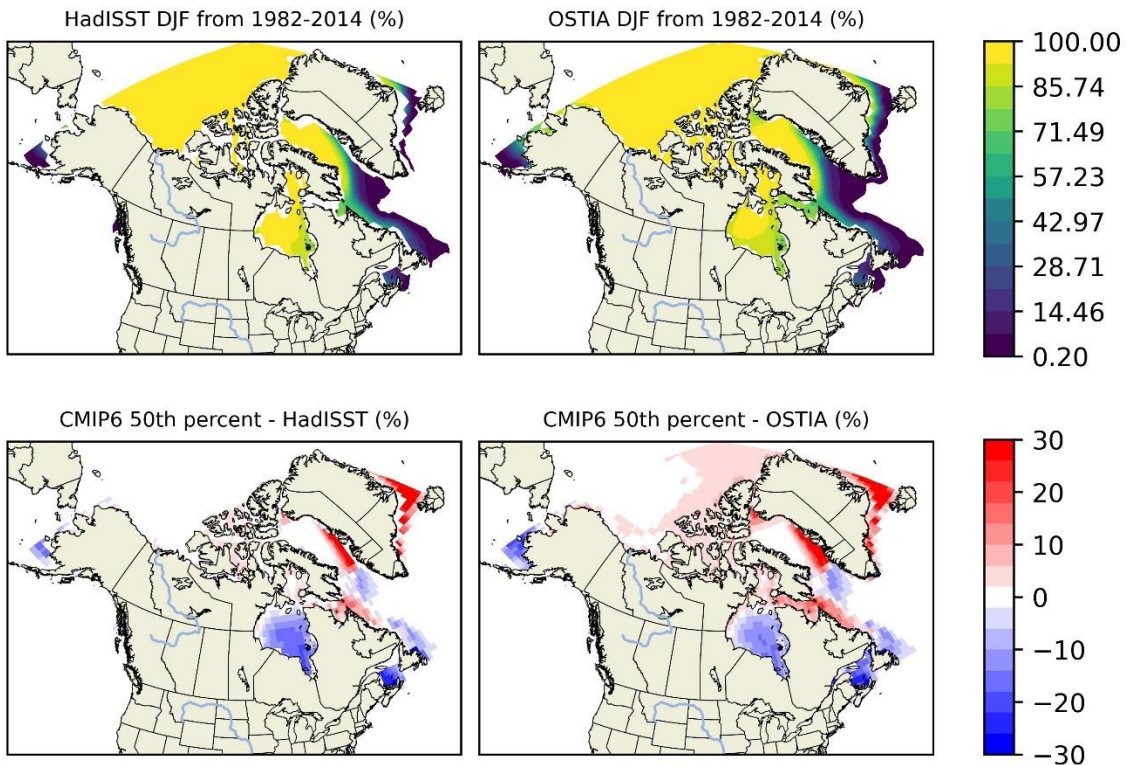


Figure 5: Spatial distribution of DJF SIC and DJF bias of the median (50th percentile) from 1982-2014. The top row shows the DJF SIC from the HadISST dataset (left) and OSTIA dataset (right). The bottom row displays the MAM bias of the median SIC from CMIP6 models relative to HadISST (left) and OSTIA (right).

4.1.2 TEMPORAL TRENDS

The yearly mean SIC trends from the CMIP6 models were compared against the observed datasets (HadISST and OSTIA) for each subregion. The comparisons were made using the median (50th), the 10th and 90th percentiles SIC from the models. The temporal trends in Gulf of St. Lawrence, Northern Newfoundland shelf, Hudson Bay as shown in the Figure 7, Figure 8 and Figure 10 respectively reveal that the CMIP6 models' median SIC underestimates the SIC compared with the yearly mean observations from HadISST and OSTIA. The range of model outputs (between the 10th and 90th percentiles) also suggests some variability in model performance, with greater spread during certain years, indicating differences in how the model handle sea ice processes and environmental conditions.

Regions such as Northern and Southern Labrador Shelf (Figure 9, Figure 11), the median model output stays close to the observed values despite the variabilities, indicating that the models capture the central tendency of SIC reasonably well. However, there are periods where the models slightly overestimate SIC compared to both datasets, particularly in the

early 1980s and late 1990. In Baffin Bay (Figure 13), the model's median shows larger deviations from both HadISST and OSTIA. The model, despite some noted underestimation (for example, 1996), tends to overestimate SIC in this region particularly during years with significant interannual variability, indicating a limitation in capturing the dynamic nature of seasonal ice changes.

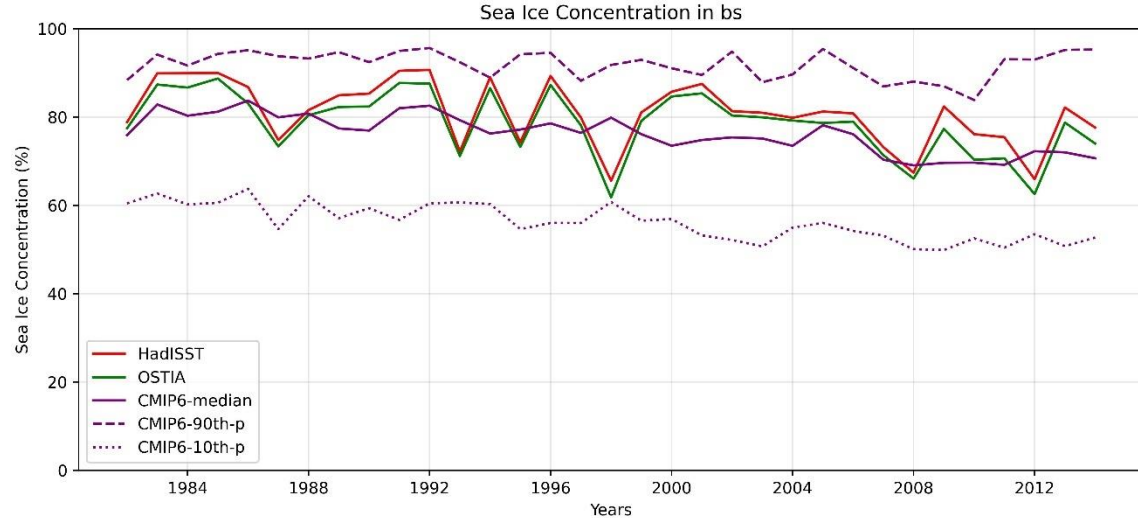


Figure 6: Modeled percentiles and observed temporal trends of yearly SIC in the Beaufort Sea from 1982 to 2014.

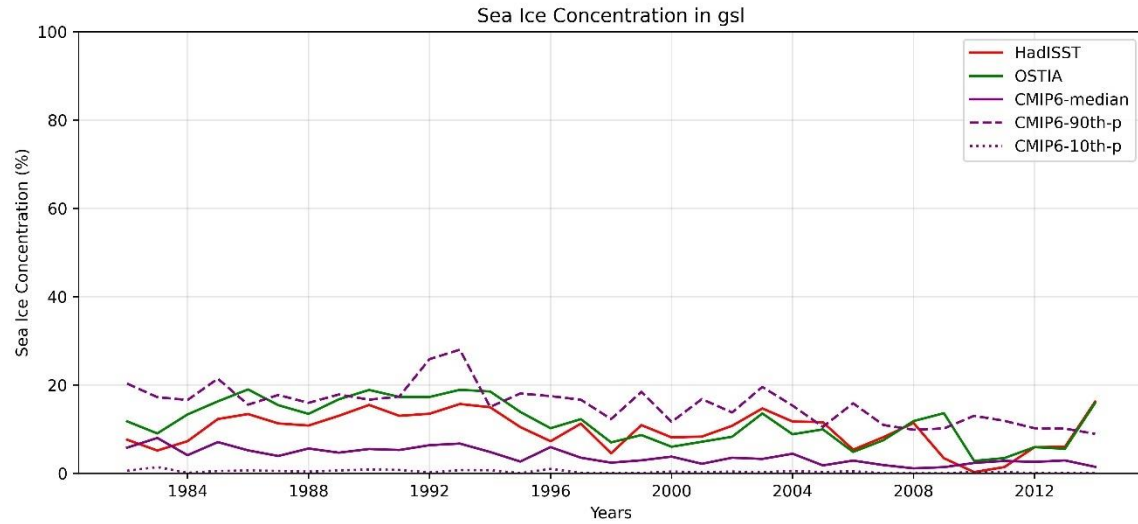


Figure 7: Modeled percentiles and observed temporal trends of yearly SIC in the Gulf of St. Lawrence from 1982 to 2014.

In other regions like the Arctic Ocean and Beaufort Sea (Figure 6, Figure 12), the CMIP6 median SIC closely matches the observed yearly mean from HadISST, showing minimal bias. This suggests that models perform better in regions with more stable ice covers.

The analysis of yearly temporal trends revealed that CMIP6 models generally captured the trends in SIC observed over the historical period. However, the trend in SIC was more closely aligned with in stable ice regions like the Arctic Ocean (ao), while discrepancies were more pronounced in variable ice regions such as the Gulf of St. Lawrence.

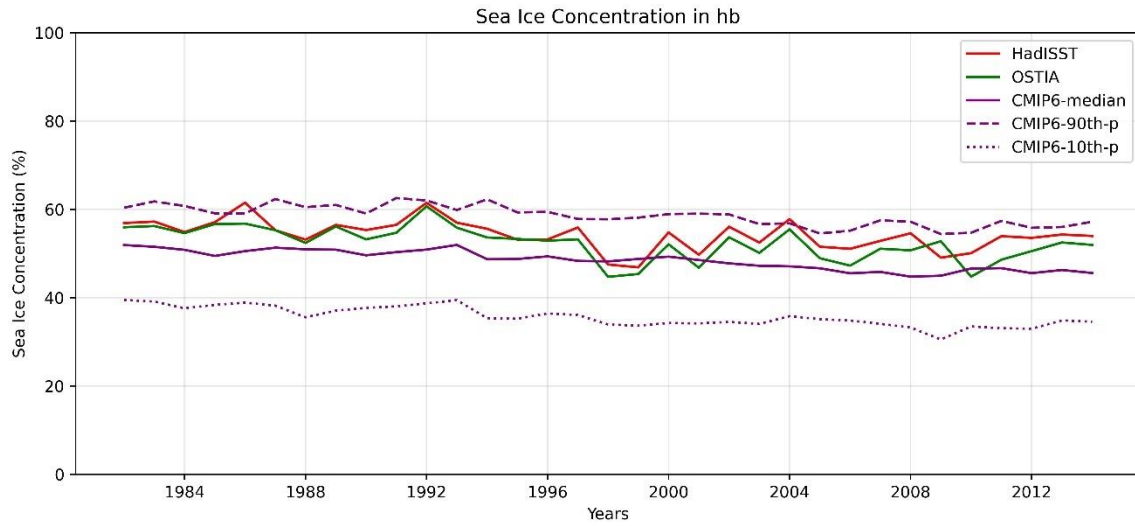


Figure 8: Modeled percentiles and observed temporal trends of yearly SIC in the Hudson Bay from 1982 to 2014.

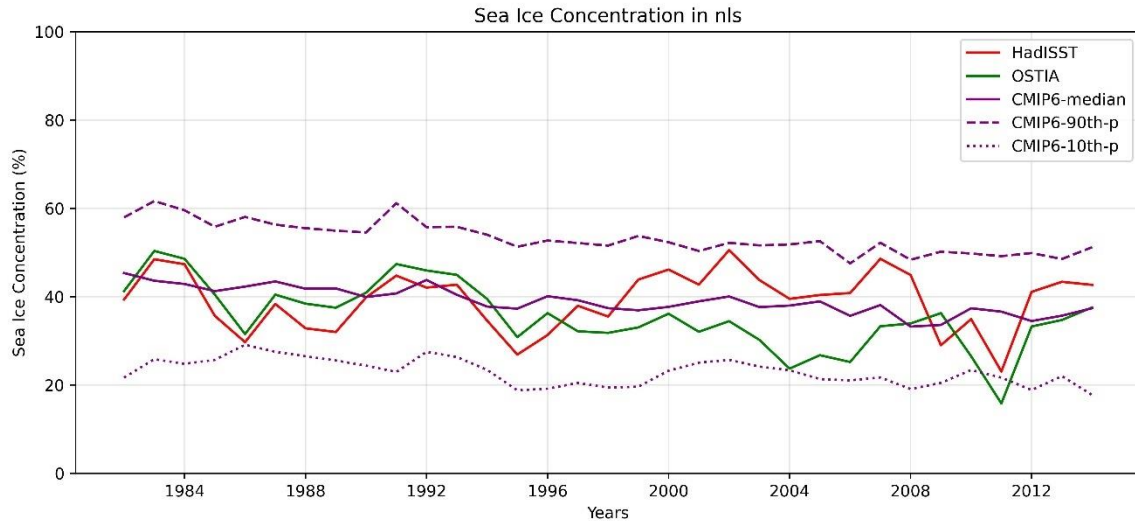


Figure 9: Modeled percentiles and observed temporal trends of yearly SIC in the Northern Labrador Shelf from 1982 to 2014.

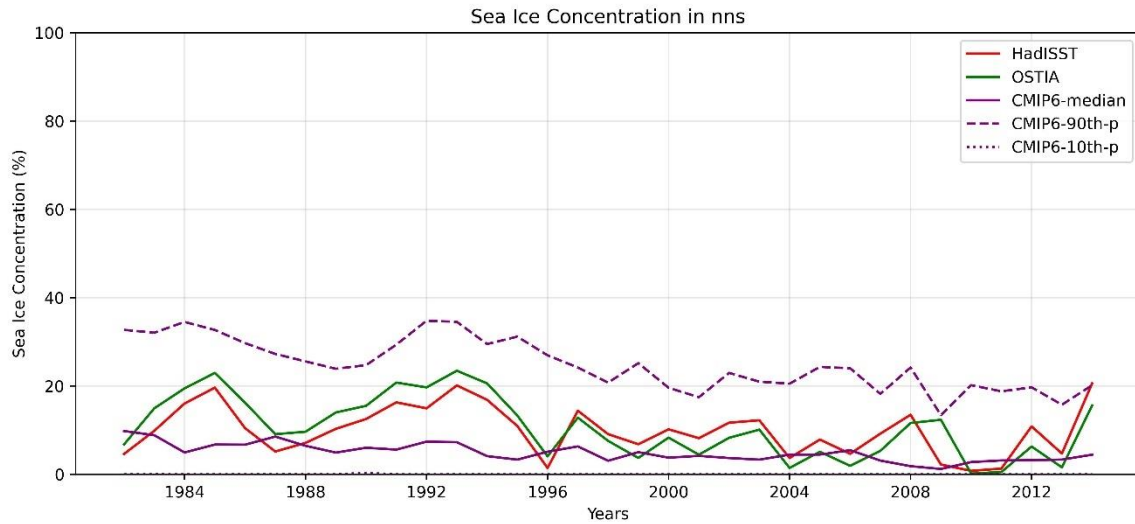


Figure 10: Modeled percentiles and observed temporal trends of yearly SIC in the Northern Newfoundland Shelf from 1982 to 2014.

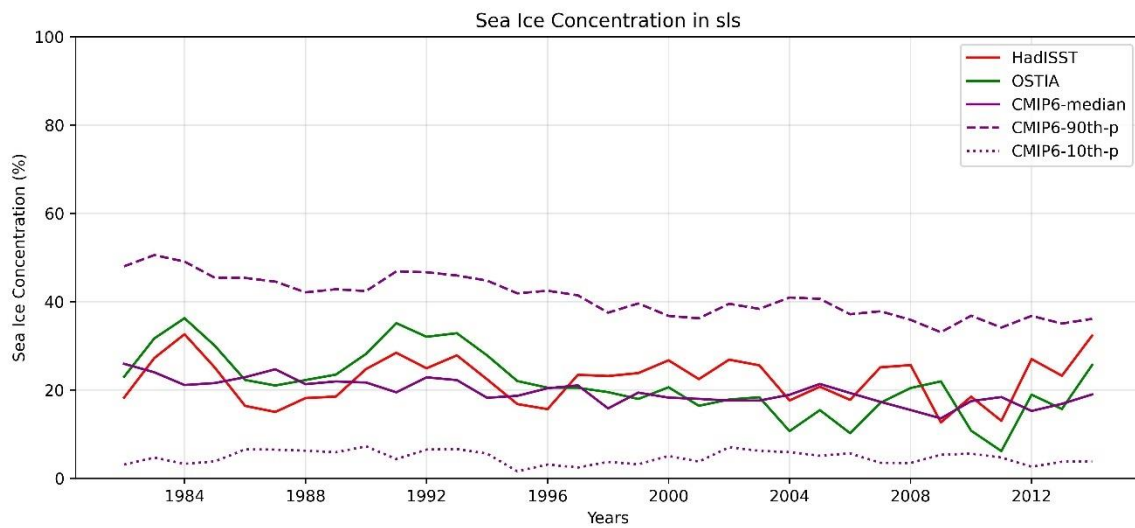


Figure 11: Modeled percentiles and observed temporal trends of yearly SIC in the Southern Newfoundland Shelf from 1982 to 2014.

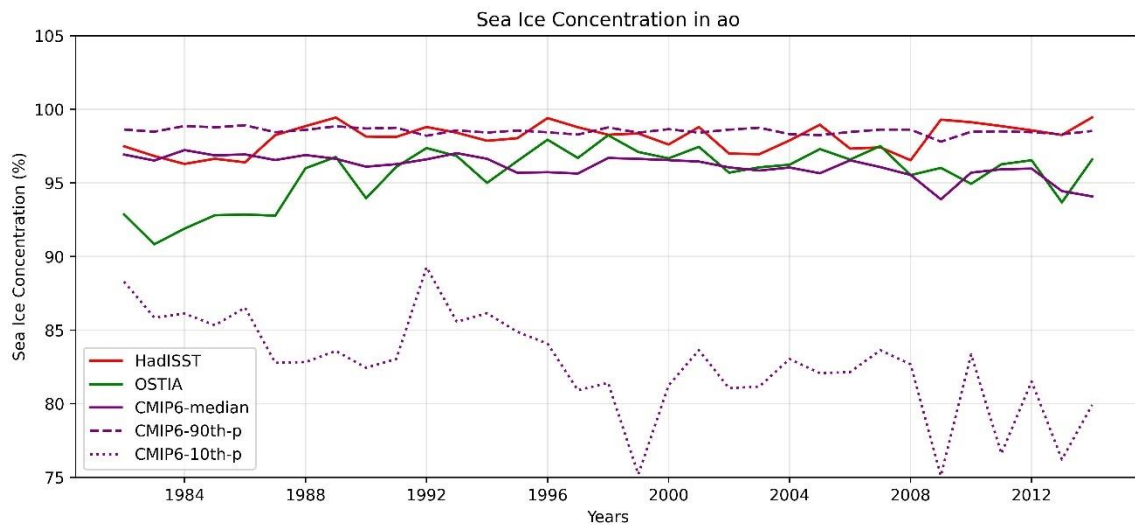


Figure 12: Modeled percentiles and observed temporal trends of yearly SIC in the Arctic Ocean Shelf from 1982 to 2014.

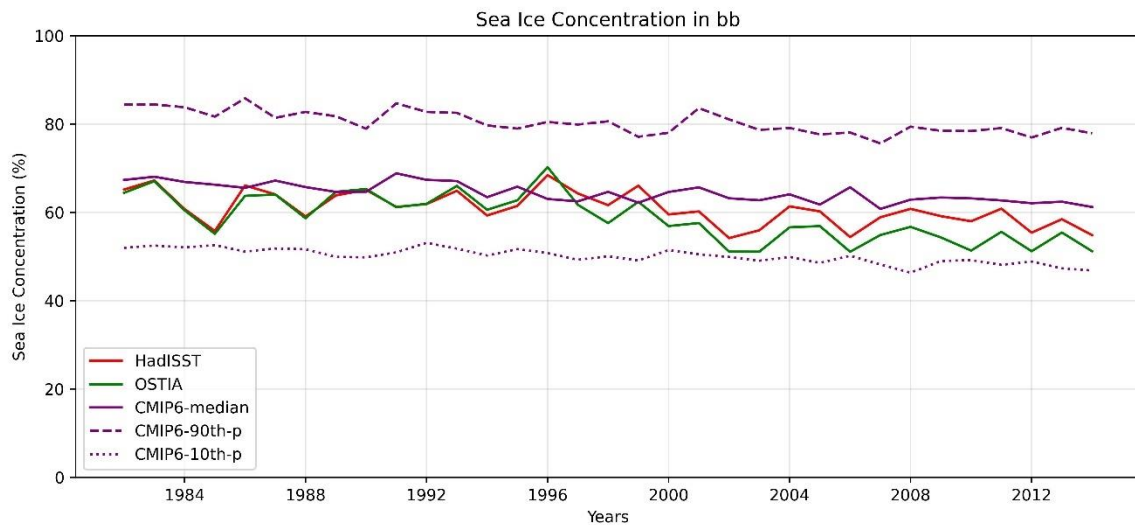


Figure 13: Modeled percentiles and observed temporal trends of yearly SIC in the Baffin Bay from 1982 to 2014.

4.2 SEA ICE THICKNESS

4.2.1 SPATIAL DISTRIBUTION

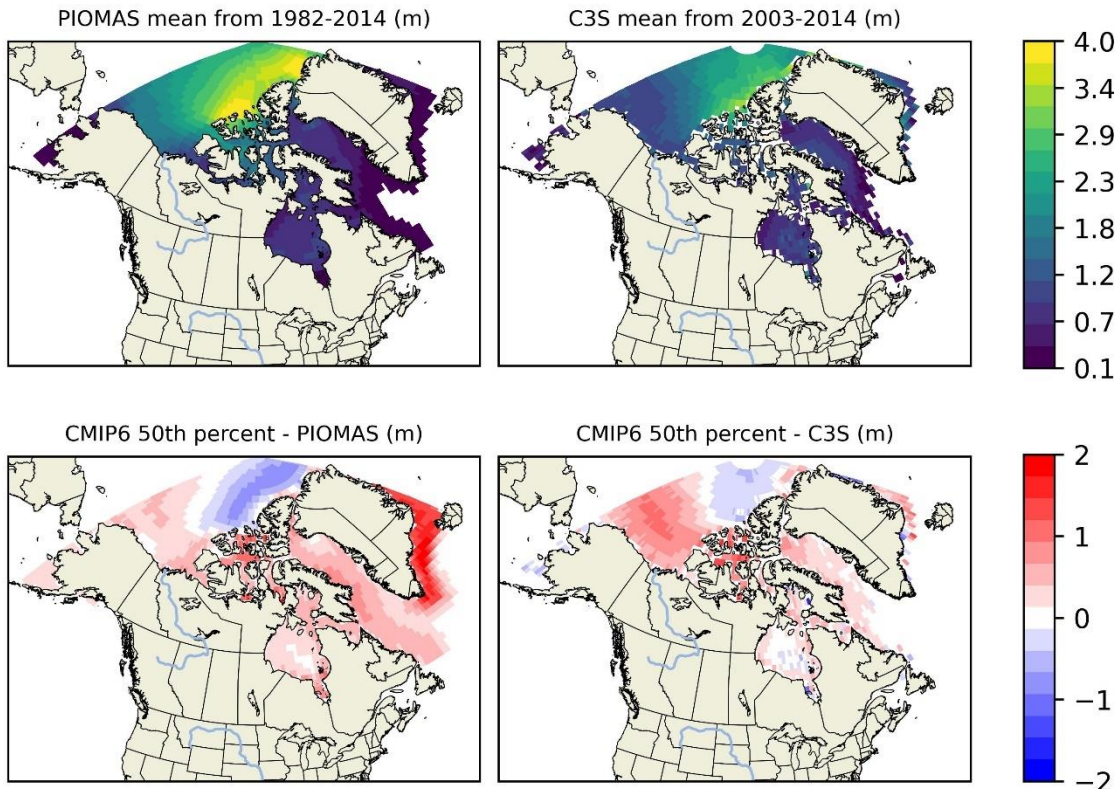


Figure 14: Spatial distribution of mean sea ice thickness (SIT) and mean bias of the median (50th percentile) from 1982-2014. The top row shows the mean SIT from the PIOMAS dataset (left) and C3S dataset (right). The bottom row displays the mean bias of the median SIT from CMIP6 models relative to PIOMAS (left) and C3S (right).

The evaluation of SIT also focused on the median (50th percentile) values to determine how well the models represent average ice thickness. The spatial distribution of the mean bias of the median SIT showed that CMIP6 models underestimated SIT in regions with thicker ice, such as the Arctic Ocean (Figure 14). When compared with PIOMAS, the models generally overestimate SIT in most regions, except for the underestimation in parts of the Arctic Ocean. However, when compared to C3S, although the models also show significant overestimations, the bias is more pronounced with PIOMAS. For example, in the southern part of Greenland, there is a very strong bias with PIOMAS, while it is less pronounced to neutral with C3S. Even for the negative bias in parts of the Arctic Ocean,

PIOMAS shows a stronger underestimation compared to C3S. This shows the model agrees poorly with PIOMAS. This discrepancy indicates that while the model shows some patches of neutral and negative bias in parts of the Arctic Ocean, they generally struggle to capture ice dynamics accurately.

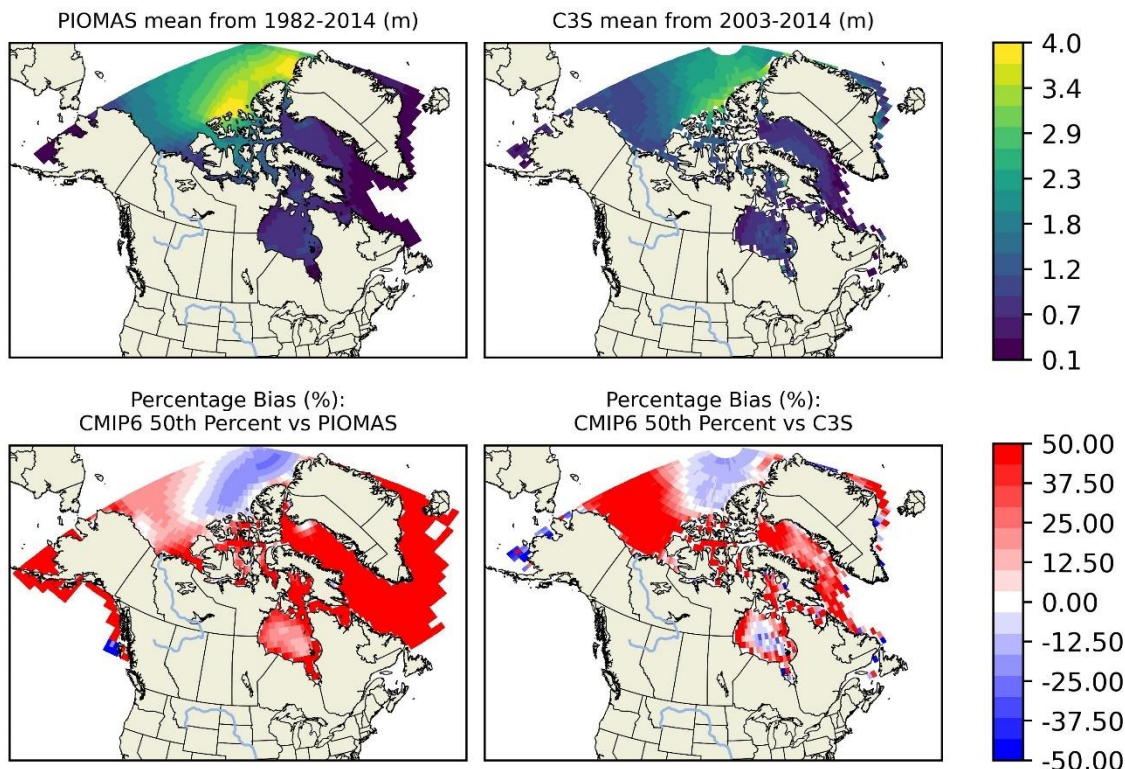


Figure 15: Spatial distribution of mean sea ice thickness (SIT) and percentage bias of the median (50th percentile) from 1982-2014. The top row shows the mean SIT from the PIOMAS dataset (left) and C3S dataset (right). The bottom row displays the percentage bias of the median SIT from CMIP6 models relative to PIOMAS (left) and C3S (right).

The percentage bias plots (Figure 15) for SIT further highlighted the challenges models face in regions with dynamic ice changes. In areas like the Labrador Sea and Baffin Bay (BB), the model showed considerable overestimations of SIT (38% to 50%) when compared to PIOMAS, suggesting difficulties in simulating ice conditions over these regions. In contrast, when compared to C3S, the model, despite showing a positive bias, exhibited less pronounced overestimations, emphasizing the importance of using multiple observational datasets to comprehensively evaluate model performance.

The seasonal plots for (Figure 16) and DJF (Figure 17) respectively indicated that models generally overestimated SIT during the spring melt season (MAM) but showed mixed performance during winter (DJF). In regions such as Hudson Bay and parts of the Arctic Ocean, underestimations were more pronounced in DJF, aligning better with C3S data. However, biases during MAM varied, reflecting the models' inconsistent ability to accurately capture the thinning phase of ice, especially when compared to PIOMAS. Interestingly, the model shows a neutral bias within the Beaufort Sea when compared to PIOMAS, while it exhibits a positive bias when compared to C3S. However, due to the large discrepancies between the model and PIOMAS, the model agrees more poorly with PIOMAS than with C3S.

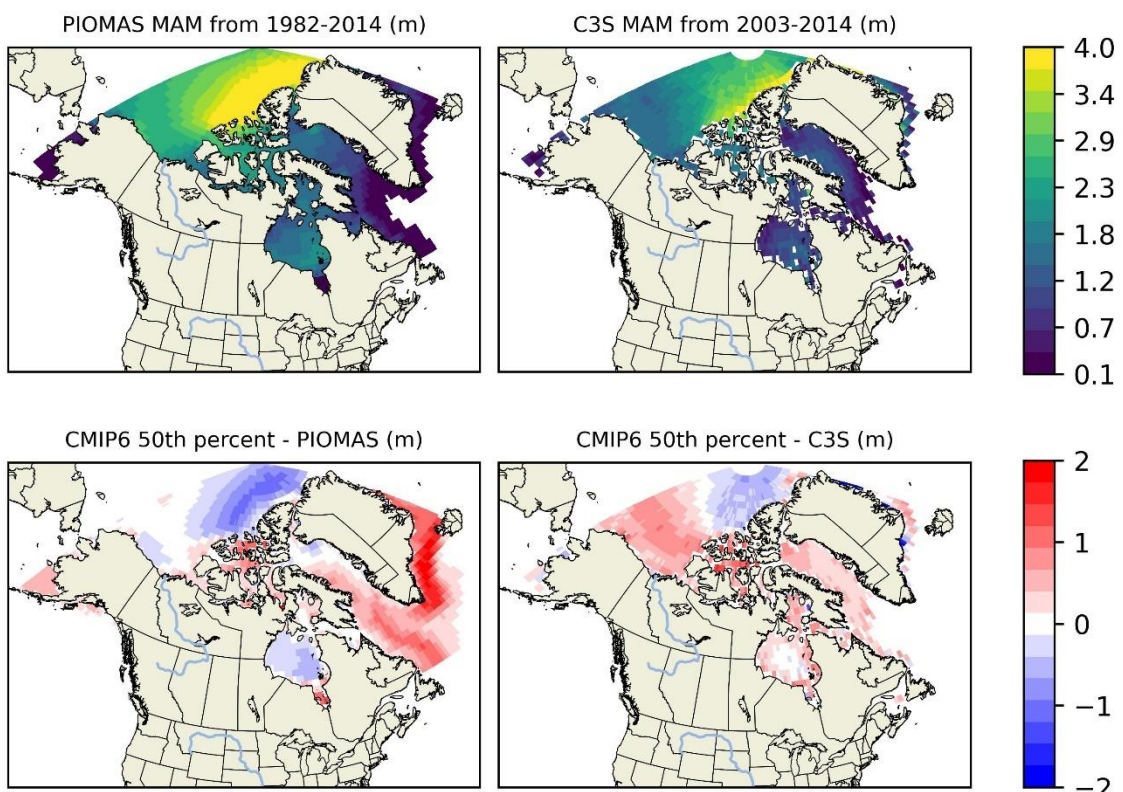


Figure 16: Spatial distribution of MAM sea ice thickness (SIT) and MAM bias of the median (50th percentile) from 1982-2014. The top row shows the MAM SIT from the PIOMAS dataset (left) and C3S dataset (right). The bottom row displays the MAM bias of the median SIT from CMIP6 models relative to PIOMAS (left) and C3S (right).

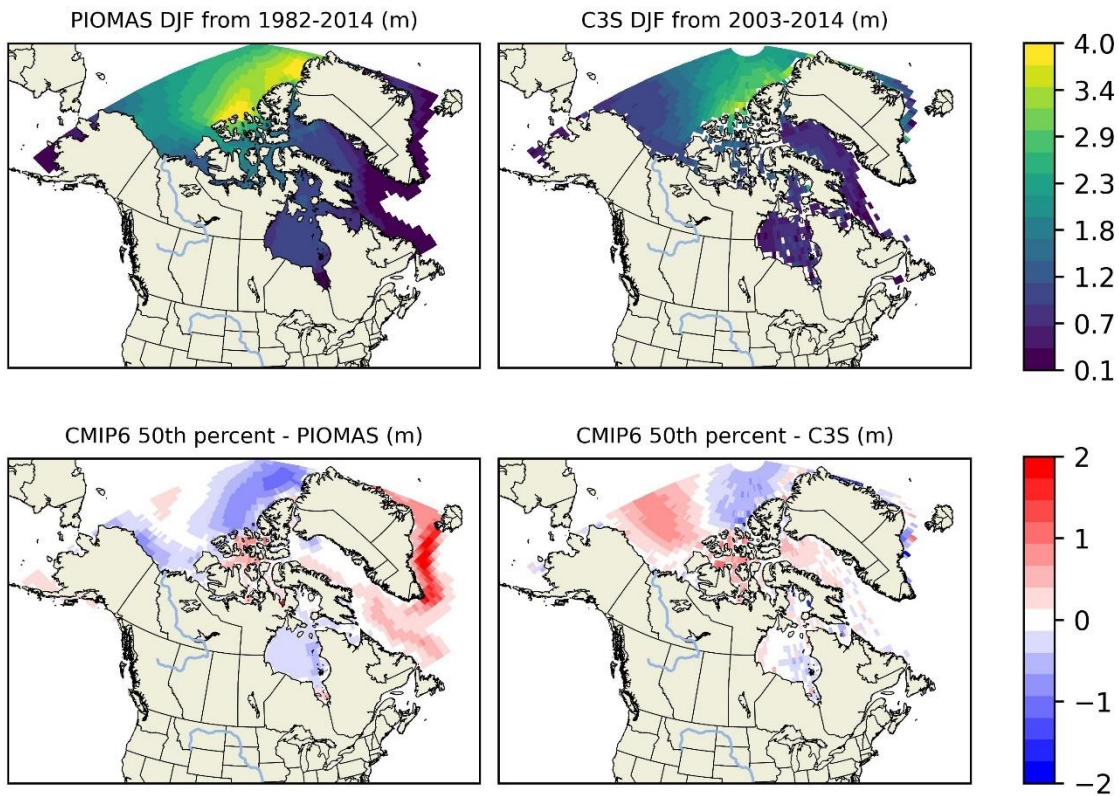


Figure 17: Spatial distribution of DJF sea ice thickness (SIT) and DJF bias of the median (50th percentile) from 1982-2014. The top row shows the DJF SIT from the PIOMAS dataset (left) and C3S dataset (right). The bottom row displays the DJF bias of the median SIT from CMIP6 models relative to PIOMAS (left) and C3S (right).

4.2.2 TEMPORAL TRENDS

The yearly mean SIT trends from CMIP6 models were compared to the observed datasets (PIOMAS and C3S) for each subregion, focusing on the median (50th percentile) SIT. In regions with thicker, multi-year ice, such as the Arctic Ocean (Figure 23), the CMIP6 models' median SIT trends are generally underestimating with both PIOMAS and C3S observations. This suggests that the model is ineffective to capture the average thickness of more stable ice regions. Also, underestimation is particularly noticeable in years with significant ice growth or during colder periods, indicating potential gaps in model representation of processes such as ice ridging and deformation. Due to unavailability of data for C3S, regions such as Gulf of St. Lawrence (Figure 19), Northern Newfoundland shelf (Figure 22) shows comparison with only PIOMAS. However, in these regions, the model tends to overestimate SIT.

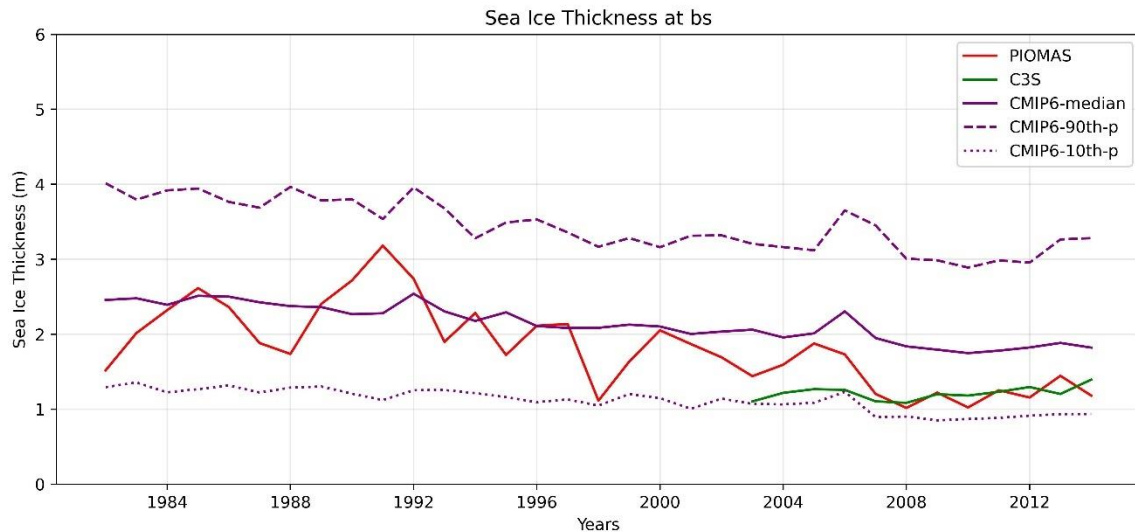


Figure 18: Modeled percentiles and observed temporal trends of yearly SIT in the Beaufort Sea from 1982 to 2014

In regions with predominantly seasonal ice, like Baffin Bay Hudson Bay (Figure 20, Figure 24) and other regions (Figure 18, Figure 21), despite the variabilities, the model shows more considerable discrepancies. The median SIT from CMIP6 models tends to overestimate the observed yearly mean SIT from both PIOMAS and C3S. This overestimation indicates that model may inadequately represent processes like ice melting and the transition between thick and thin ice states, leading to biases in regions with dynamic ice conditions. The only pronounced underestimation was observed in Southern Labrador shelf (Figure 25) temporal trend where the model's median SIT underestimated C3S data in 2005.

The comparison with different observational datasets (PIOMAS and C3S) for SIT reveals that model performance can vary significantly depending on the data used for validation. PIOMAS, which integrates observational data with a numerical model, tends to show poor agreement with the CMIP6 median SIT in regions with thicker ice. Similarly, C3S highlights discrepancies in ice regions, suggesting that models generally agrees poorly with the observations.

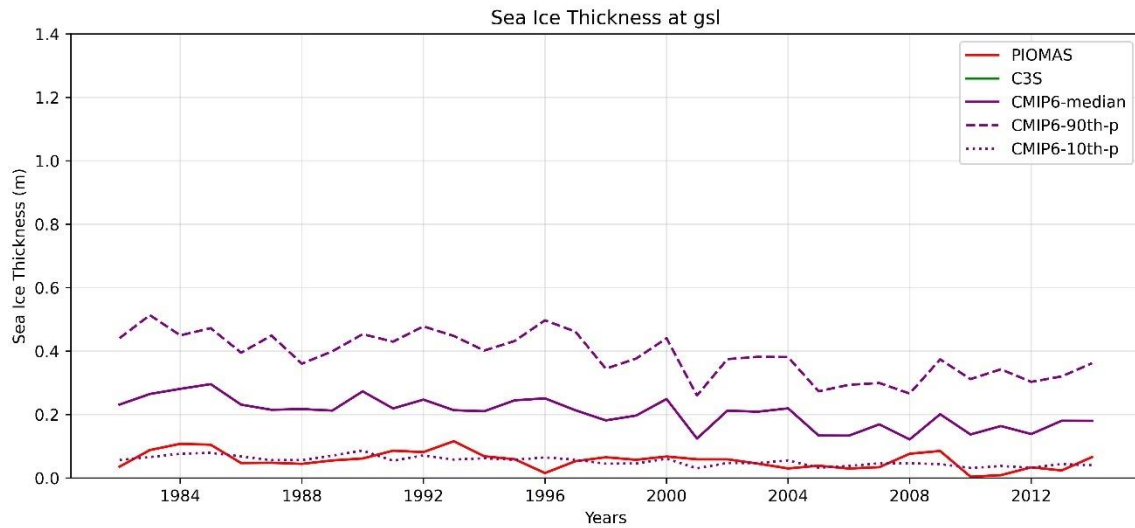


Figure 19: Modeled percentiles and observed temporal trends of yearly SI in the Gulf of St. Lawrence from 1982 to 2014.

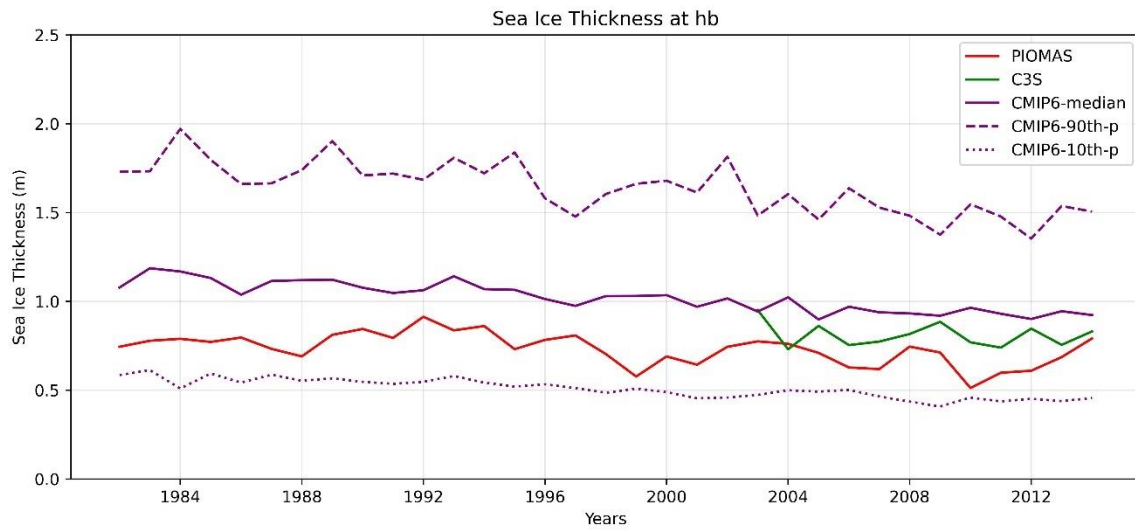


Figure 20: Modeled percentiles and observed temporal trends of yearly SIT in the Hudson Bay from 1982 to 2014

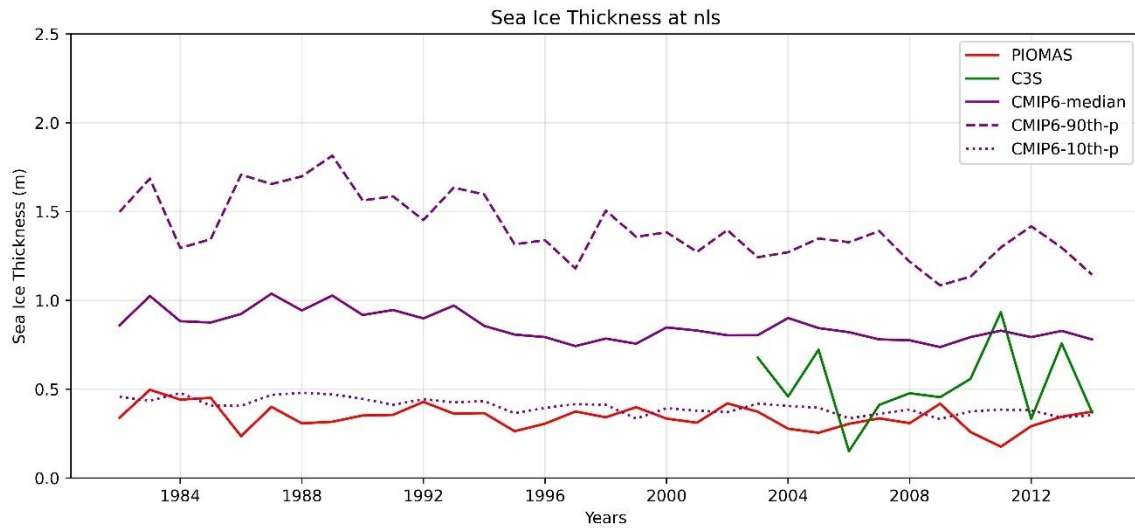


Figure 21: Modeled percentiles and observed temporal trends of yearly SIT in the Northern Labrador Shelf from 1982 to 2014.

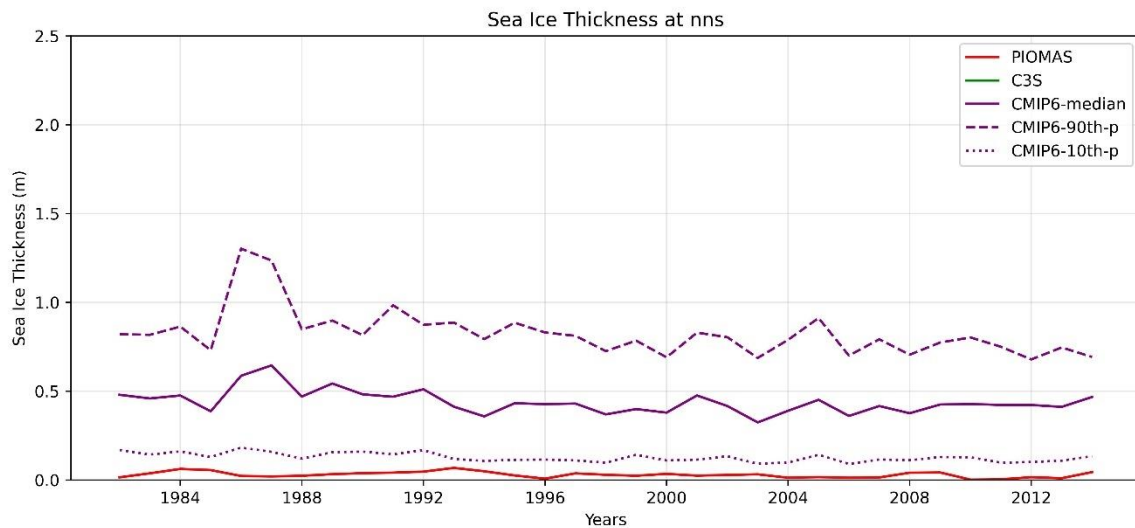


Figure 22: Modeled percentiles and observed temporal trends of yearly SIT in the Northern Newfoundland Shelf from 1982 to 2014.

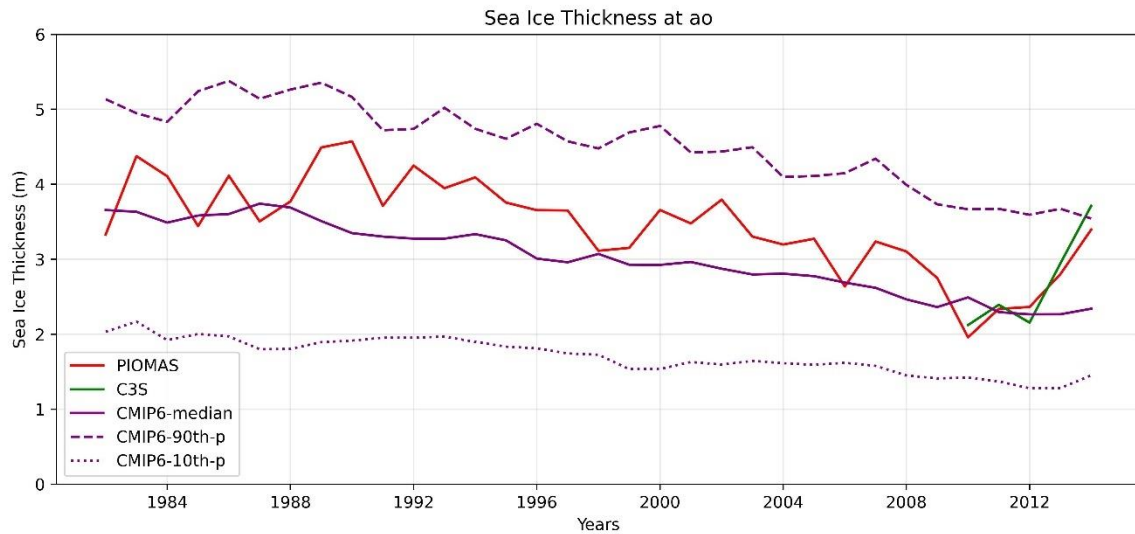


Figure 23: Modeled percentiles and observed temporal trends of yearly SIT in the Arctic Ocean Shelf from 1982 to 2014.

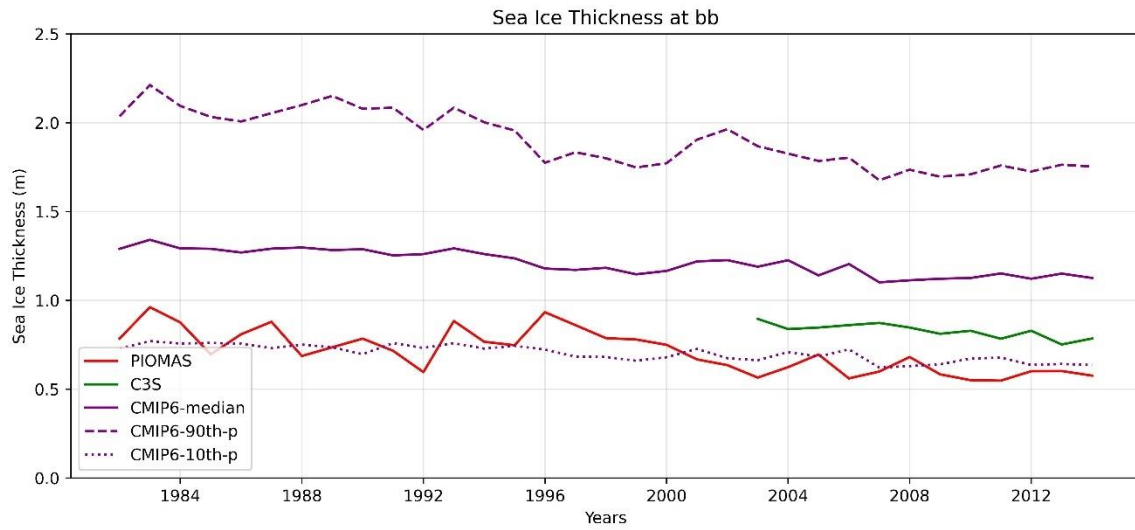


Figure 24: Modeled percentiles and observed temporal trends of yearly SIT in the Baffin Bay Shelf from 1982 to 2014

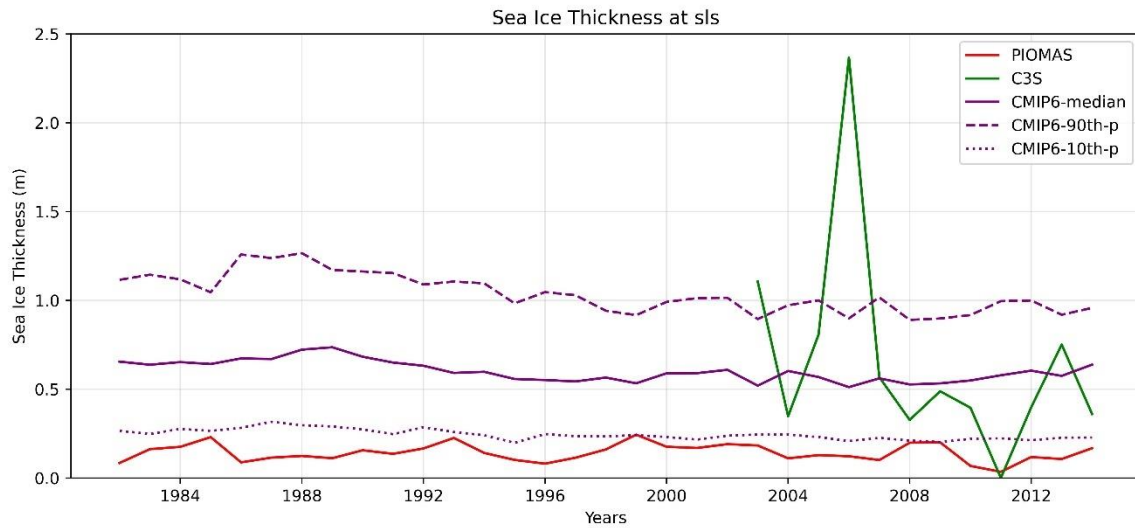


Figure 25: Modeled percentiles and observed temporal trends of yearly SIT in the Southern Labrador Shelf from 1982 to 2014

5 DISCUSSION

The results of this assessment highlight several important considerations for understanding and improving CMIP6 models' simulations of sea ice concentration and thickness. The observed biases in SIC and SIT across different subregions and seasons suggest that while CMIP6 models are generally effective at capturing large-scale sea ice trends, there are significant challenges in accurately simulating regional and seasonal variability. These biases are likely due to differences in model resolution, sea ice dynamics, and thermodynamic processes such as melt ponds, ice ridging, and snow-ice interactions.

Although the models captured some trends in SIC and SIT for certain regions, such as the Arctic Ocean, the strong overestimation consistently observed over the southern part of Greenland indicates the models' inability to capture the local effects of topography, ocean, and atmospheric circulation in that region. Additionally, the biases in model performance across different subregions emphasize the need for further analysis to have confidence in the robustness of the models. Incorporating higher-resolution observational data into model evaluations could help identify specific areas for improvement.

While CMIP6 models provide valuable insights into sea ice behavior around Canada, there are clear areas where model performance can be enhanced. Focusing on reducing biases and improving the representation of sea ice processes will be essential for increasing the reliability of future sea ice projections, particularly in the context of a changing climate.

6 CONCLUSION

The evaluation of CMIP6 models in simulating sea ice concentration (SIC) and sea ice thickness (SIT) across the eight subregions around Canada provides valuable insights into the models' strengths and areas needing improvement. By focusing on the 50th percentile (median) values, this assessment highlights how well the models represent typical sea ice conditions and their variability over time.

Key Findings:

1. CMIP6 models generally perform well in regions with stable, multi-year ice, such as the Arctic Ocean, where the median model sea ice concentration outputs closely align with observational datasets (HadISST and PIOMAS).
2. In regions with more dynamic, seasonal ice cover, such as Hudson Bay, Baffin Bay, and the Gulf of St. Lawrence, the models exhibit more significant biases and variability, particularly in capturing the transitional phases of ice melt and formation.
3. The comparison against C3S for SIT showed a high overestimation, indicating poor agreement between the model and the observations.
4. CMIP6 exhibited improved performance in sea ice concentration (SIC) when compared to HadISST relative to OSTIA. Similarly, CMIP6 demonstrated good performance in sea ice thickness (SIT) with C3S compared to PIOMAS, despite the biases.
5. The CMIP6 models show a large positive bias in the southern part of Greenland for both SIC and SIT due to the inability of the model to fully capture the influence of local topography, ocean currents, and atmospheric circulation in the region.
6. Overall, CMIP6 models exhibit smaller biases for sea ice concentration, particularly in the Arctic Ocean. However, further analysis may be required to draw conclusions on sea ice thickness, including comparisons with other datasets.

7 DATA AVAILABILITY

The observed datasets used in this study for both the sea ice concentration and thickness, which are HadISST, OSTIA, PIOMAS and C3S, are publicly available and can be accessed from their respective sources: HadISST from the Met Office Hadley Centre ([SST data: HadISST v1.1 | Climate Data Guide \(ucar.edu\)](#)), OSTIA from the Copernicus Marine Environment Monitoring Service ([Global Ocean OSTIA Sea Surface Temperature and Sea Ice Reprocessed | Copernicus Marine Service](#)), PIOMAS from the Polar Science Center at the University of Washington ([Polar Science Center » PIOMAS Variables on Model Grid \(uw.edu\)](#)), and C3S from the Copernicus Climate Data Store ([Arctic Ocean - Sea Ice Thickness REPROCESSED | Copernicus Marine Service](#)).

8 BIBLIOGRAPHY

- Barber, D. G., Asplin, M. G., Raddatz, R. L., Candlish, L. M., Nickels, S., Meakin, S., . . . Prinsenberg, S. J. (2012). Change and variability in sea ice during the 2007–2008 Canadian International Polar Year program. *Climatic Change*, 115, 115–133. Retrieved from <https://doi.org/10.1007/s10584-012-0477-6>
- Bhatt, U. S., Walker, D. A., Walsh, J. E., Carmack, E. C., Frey, K. E., Meier, W. N., . . . others, a. (2014). Implications of Arctic sea ice decline for the Earth system. *Annual Review of Environment and Resources*, 39, 57–89. Retrieved from <https://doi.org/10.1146/annurev-environ-122012-094357>
- Döscher, R., Vihma, T., & Maksimovich, E. (2014). Recent advances in understanding the Arctic climate system state and change from a sea ice perspective: a review. 14, pp. 13571–13600. Retrieved from <https://doi.org/10.5194/acp-14-13571-2014>
- Good, S., Fiedler, E., Mao, C., Martin, M. J., Maycock, A., Reid, R., & Roberts-Jones, J. (2020). The Current Configuration of the OSTIA System for Operational Production of Foundation Sea Surface Temperature and Ice Concentration Analyses. *Remote Sensing*, 12, no. 4: 720. Retrieved from <https://doi.org/10.3390/rs12040720>
- Henke, M., Cassalho, F., Miesse, T., Ferreira, C. M., Zhang, J., & Ravens, T. M. (2023). Assessment of Arctic sea ice and surface climate conditions in nine CMIP6 climate models. *Arctic, Antarctic, and Alpine Research*, 2271592. Retrieved from <https://doi.org/10.1080/15230430.2023.2271592>
- Post, E., Bhatt, U. S., Bitz, C. M., Brodie, J. F., Fulton, T. L., Hebblewhite, M., . . . Walker, D. A. (2013). Ecological consequences of sea-ice decline. *Science*, 341, 519–524. Retrieved from <https://doi.org/10.1126/science.1235225>

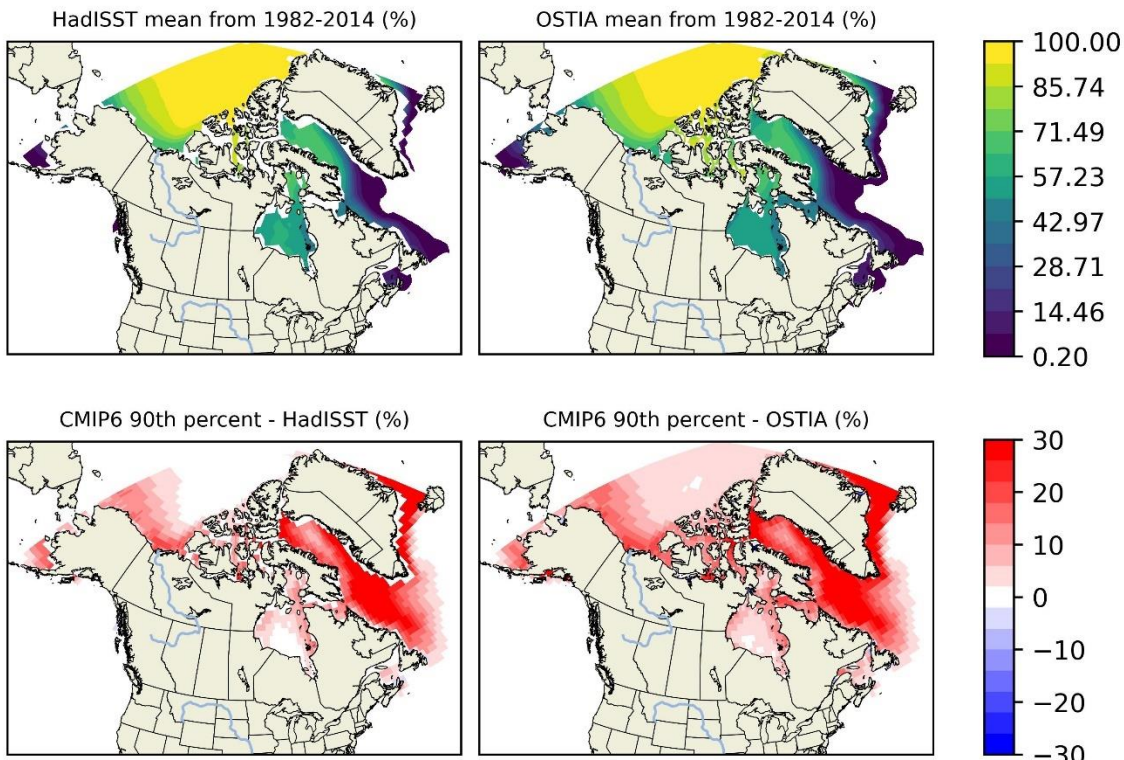
- Rayner, N. A., Parker, D. E., Horton, E. B., Folland, C. K., Alexander, L. V., Rowell, D. P., . . . Kaplan, A. (2003). Global analyses of sea surface temperature, sea ice, and night marine air temperature since the late nineteenth century. *Journal of Geophysical Research: Atmospheres*, 108, no. D14. Retrieved from <https://doi.org/10.1029/2002JD002670>
- Schweiger, A., Lindsay, R., Zhang, J., Steele, M., Stern, H., & Kwok, R. (2011). Uncertainty in modeled Arctic sea ice volume. *Journal of Geophysical Research: Oceans*, 116, no. C8 . Retrieved from <https://doi.org/10.1029/2011JC007084>
- Vihma, T. (2014). Effects of Arctic sea ice decline on weather and climate: A review. *Surveys in Geophysics*, 35, 1175-1214. Retrieved from <https://doi.org/10.1007/s10712-014-9284-0>
- Zhang, J., & Rothrock, D. A. (2003). Modeling global sea ice with a thickness and enthalpy distribution model in generalized curvilinear coordinates. *Monthly Weather Review*, 131, 845-861. Retrieved from [https://doi.org/10.1175/1520-0493\(2003\)131%3C0845:MGSIWA%3E2.0.CO;2](https://doi.org/10.1175/1520-0493(2003)131%3C0845:MGSIWA%3E2.0.CO;2)

9 APPENDIX

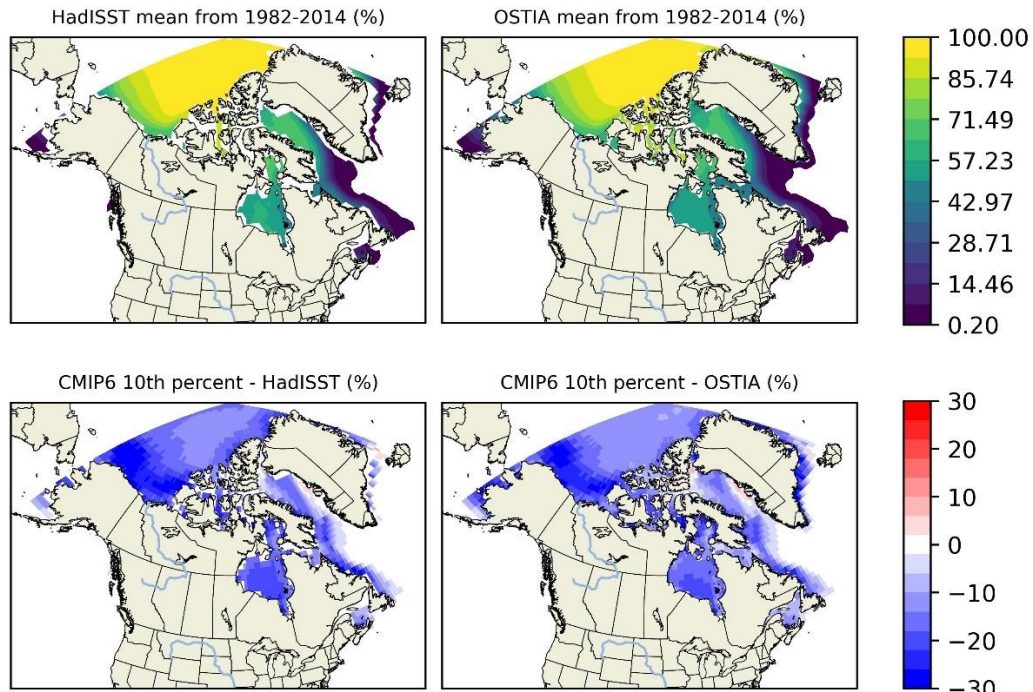
The appendix contains detailed analyses of the 10th and 90th percentiles for both SIT and SIC, as well as the seasonal bias plots for the remaining seasons (JJA - June, July, August; SON - September, October, November). These supplementary materials provide a more comprehensive view of model performance across a wider range of sea ice conditions and further explore the models' abilities to capture extreme states and seasonal transitions.

9.1 SIC

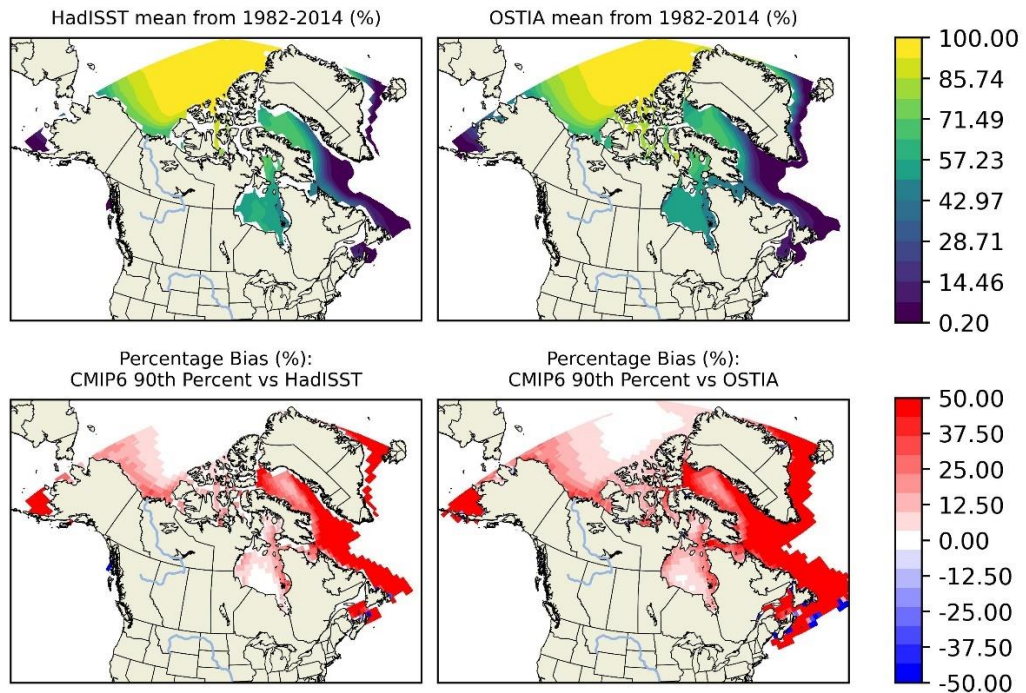
- SIC mean and mean bias of 90th Percentile (1982-2014)



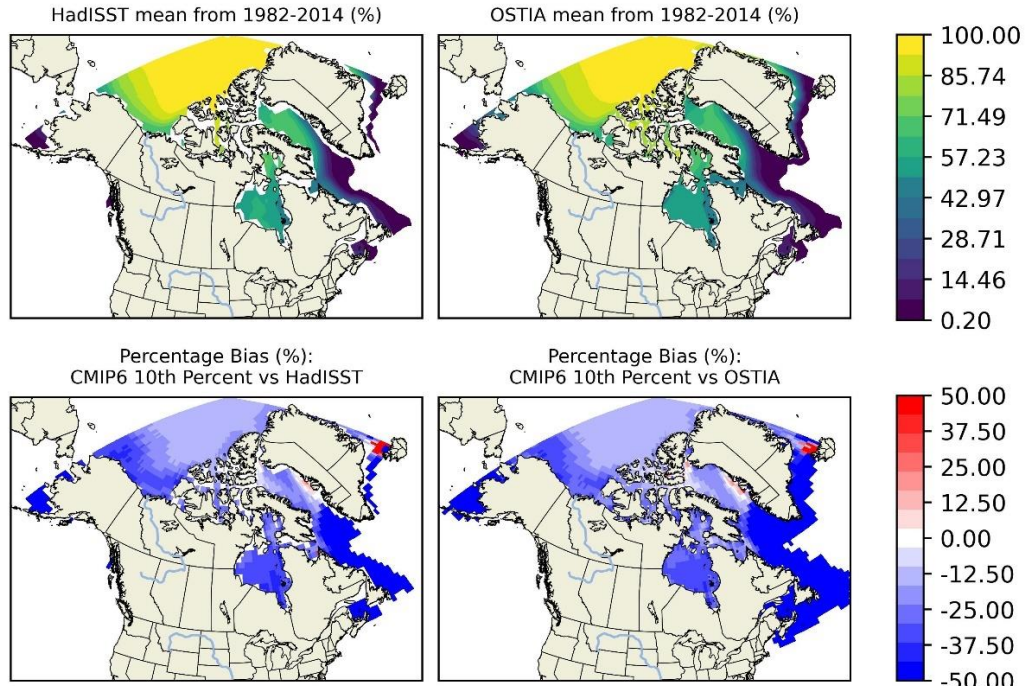
- SIC mean and mean bias of 10th Percentile (1982-2014)



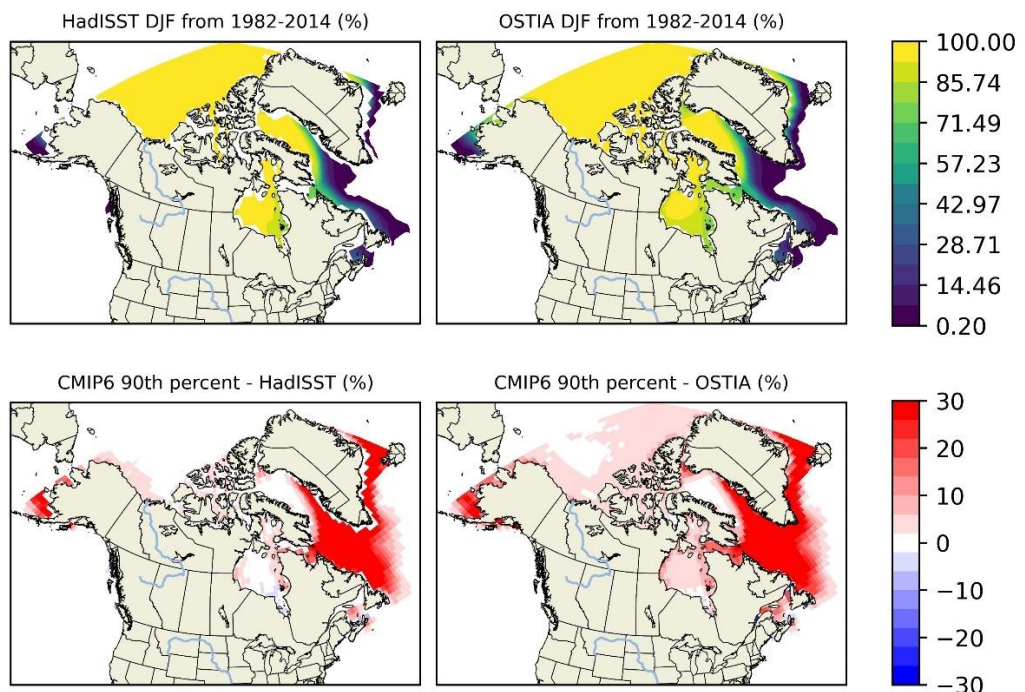
- SIC mean and percentage bias of 90th Percentile (1982-2014)



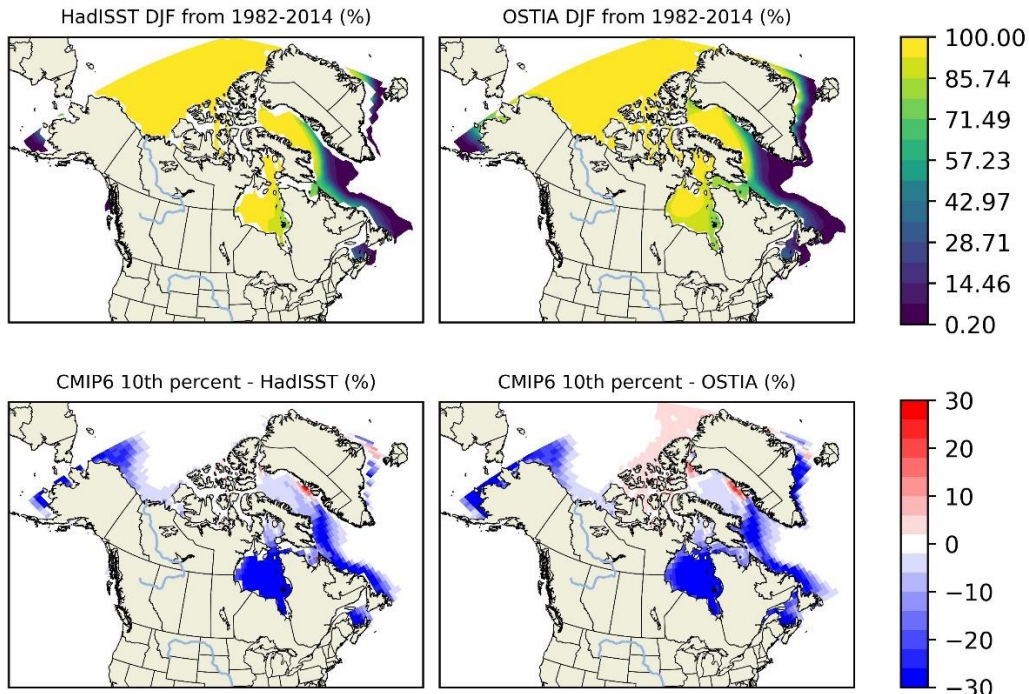
- SIC mean and percentage bias of 10th Percentile (1982-2014)



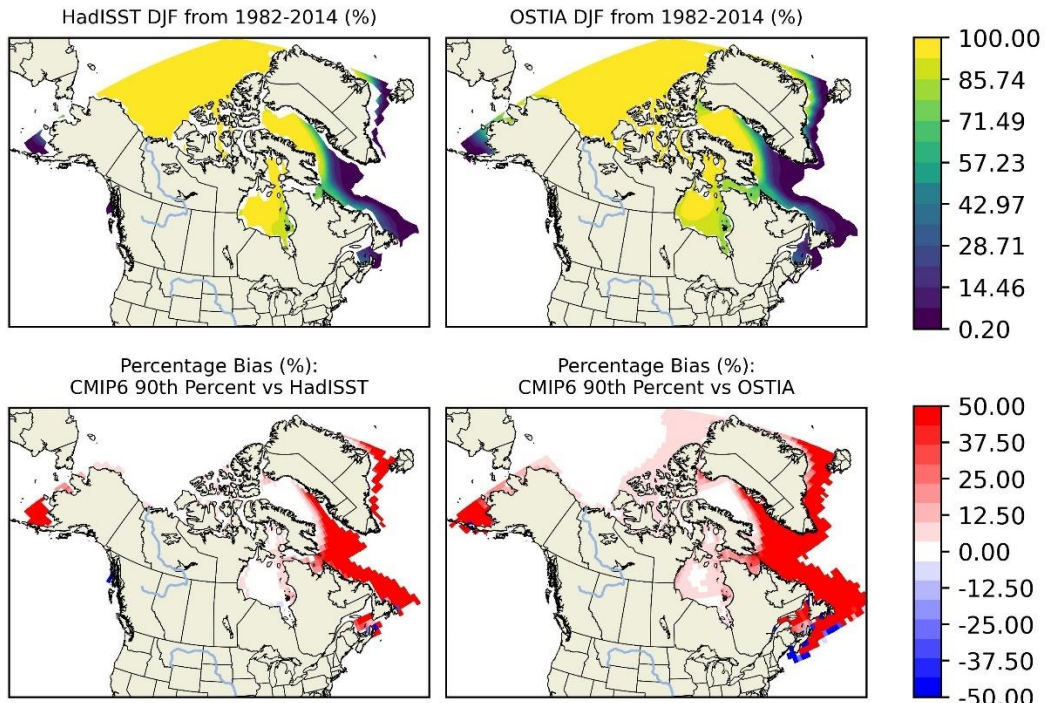
- SIC DJF and DJF bias of 90th Percentile (1982-2014)



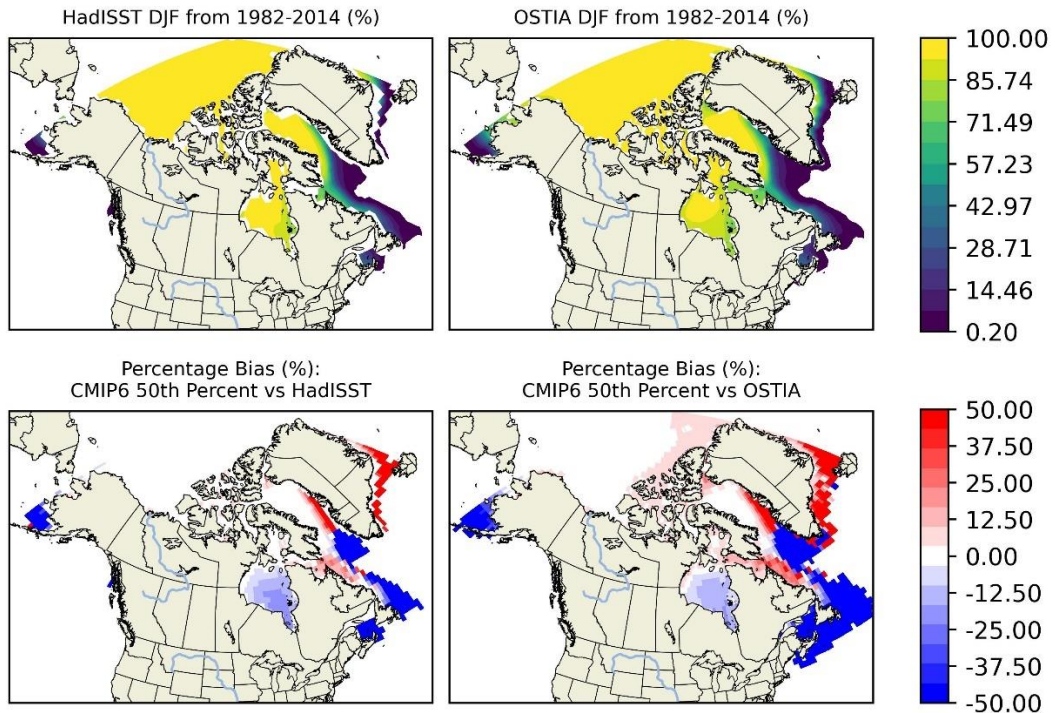
- SIC DJF and DJF bias of 10th Percentile (1982-2014)



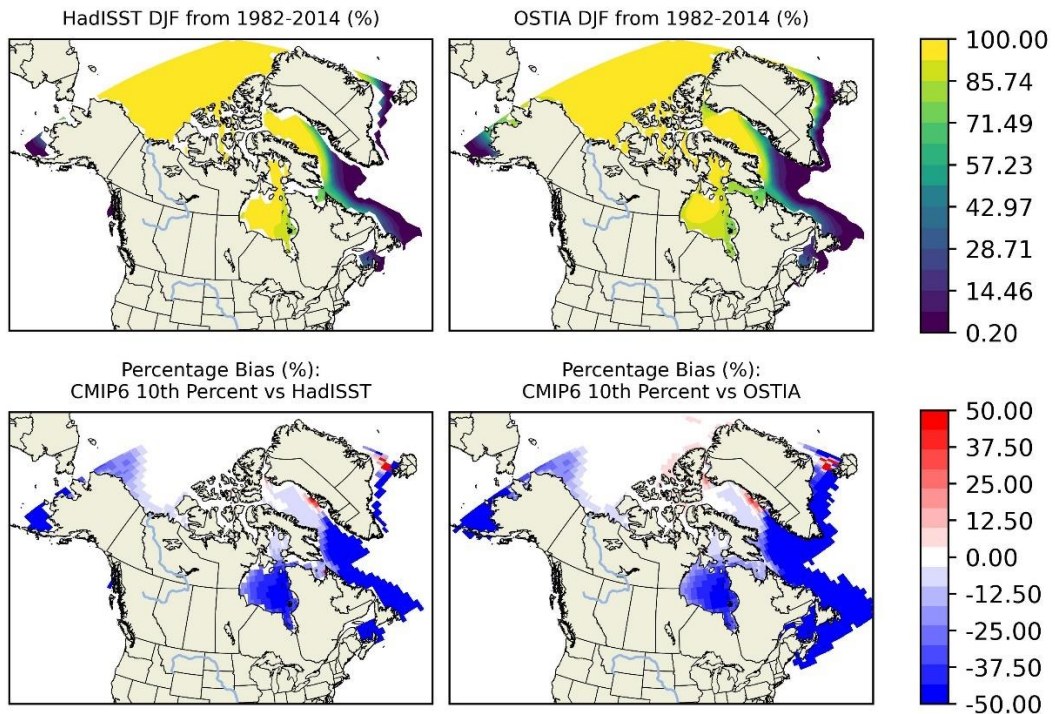
- SIC DJF and DJF percentage bias of 90th Percentile (1982-2014)



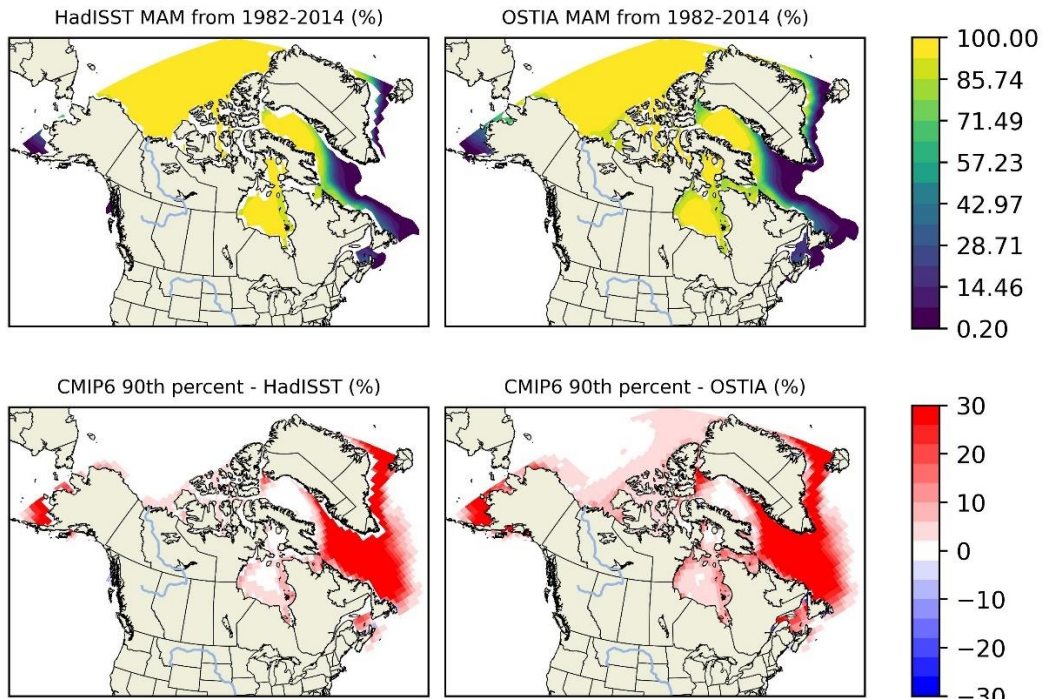
- SIC DJF and DJF percentage bias of 50th Percentile (1982-2014)



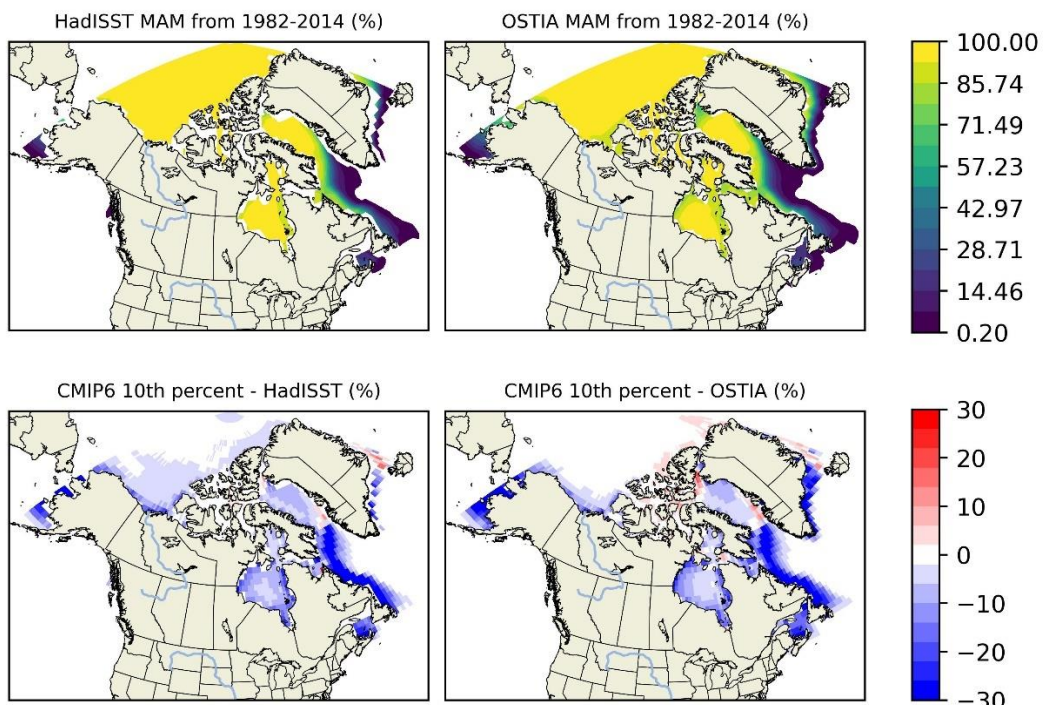
- SIC DJF and DJF percentage bias of 10th Percentile (1982-2014)



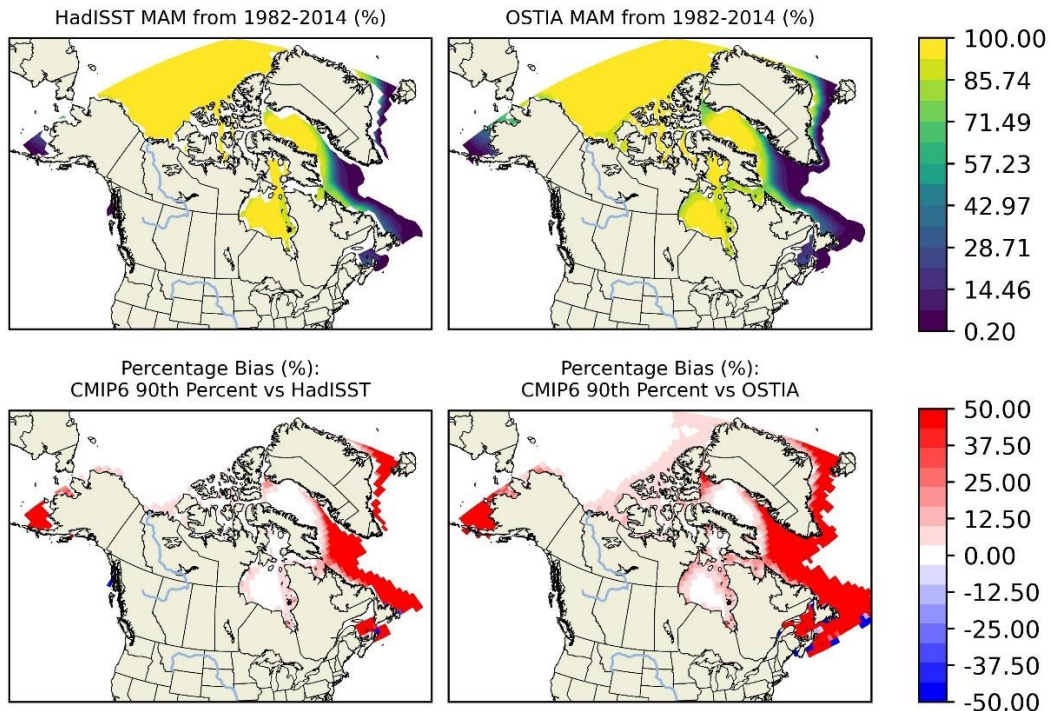
- SIC MAM and MAM bias of 90th Percentile (1982-2014)



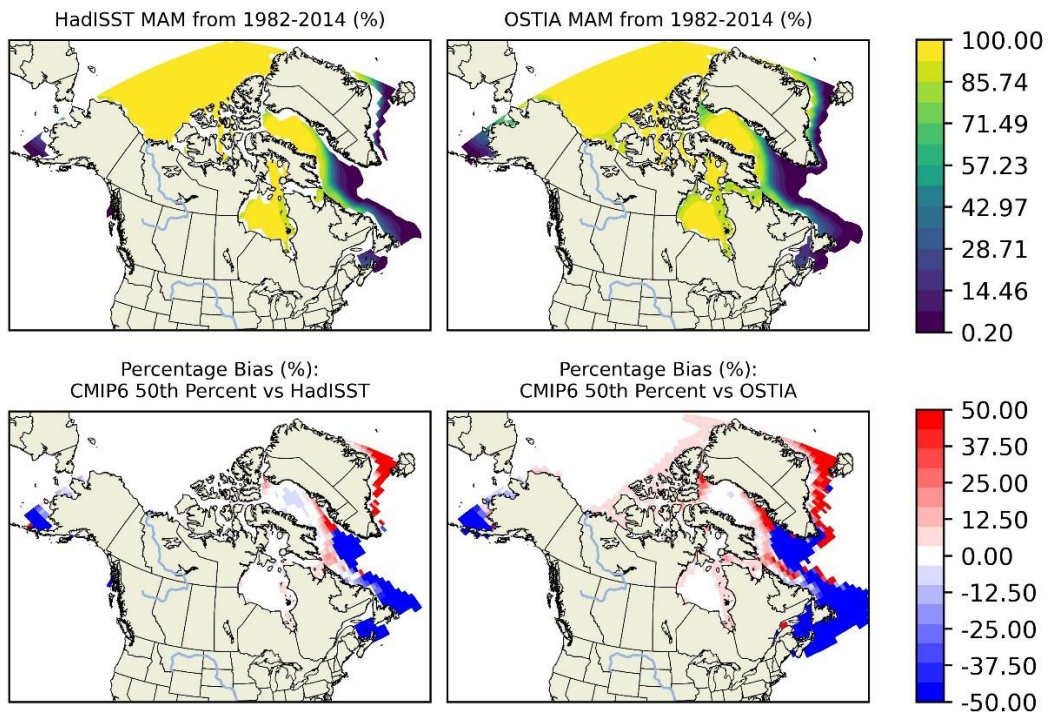
- SIC MAM and MAM bias of 10th Percentile (1982-2014)



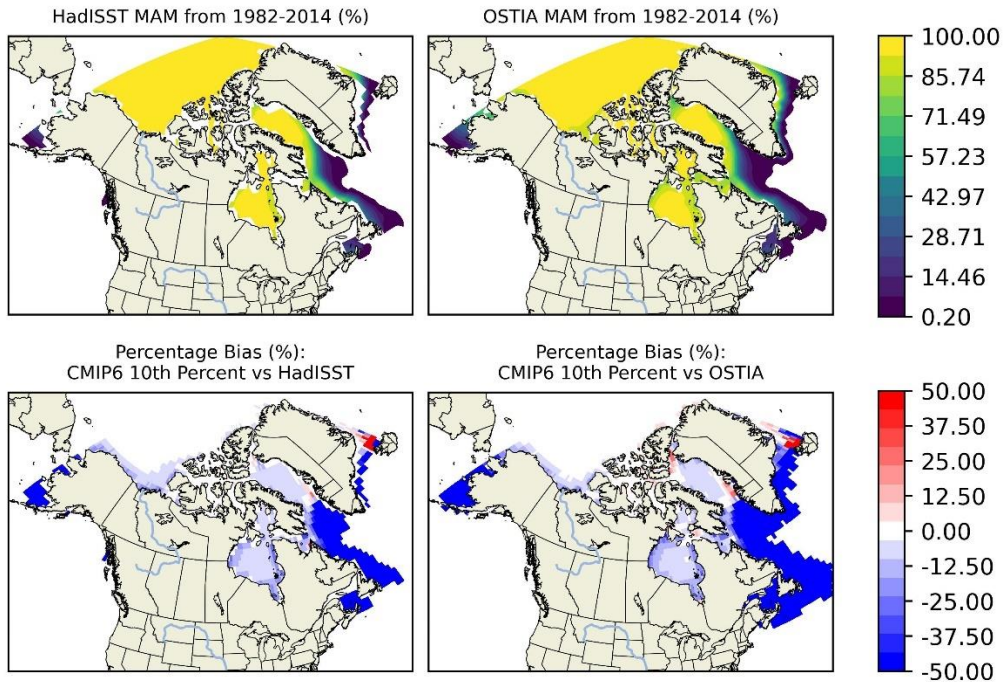
- SIC MAM and MAM percentage bias of 90th Percentile (1982-2014)



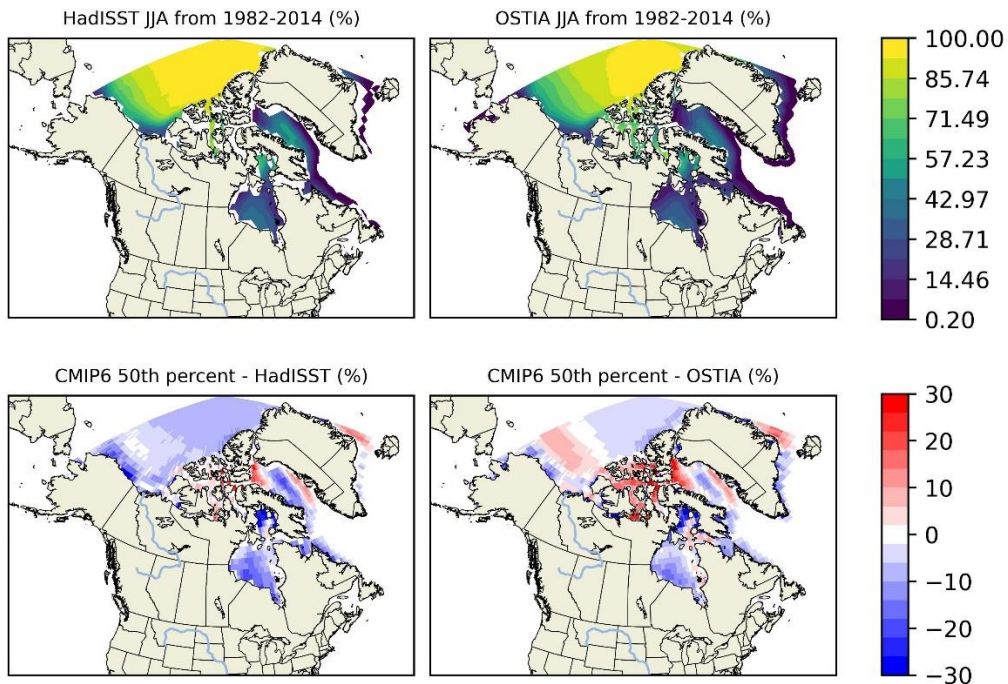
- SIC MAM and MAM percentage bias of 50th Percentile (1982-2014)



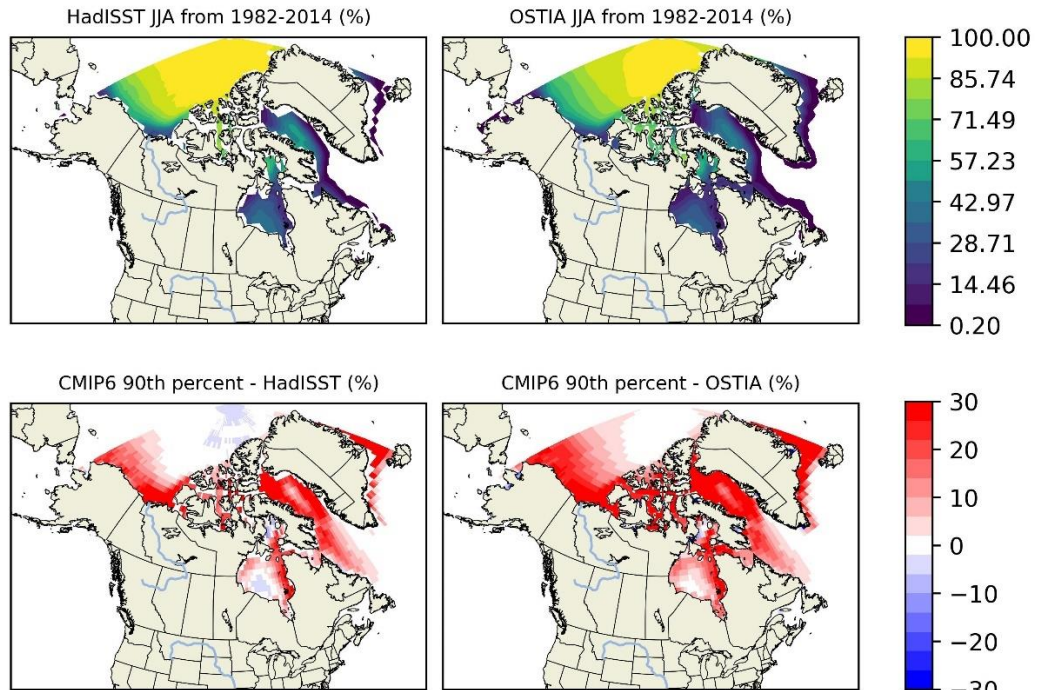
- SIC MAM and MAM percentage bias of 10th Percentile (1982-2014)



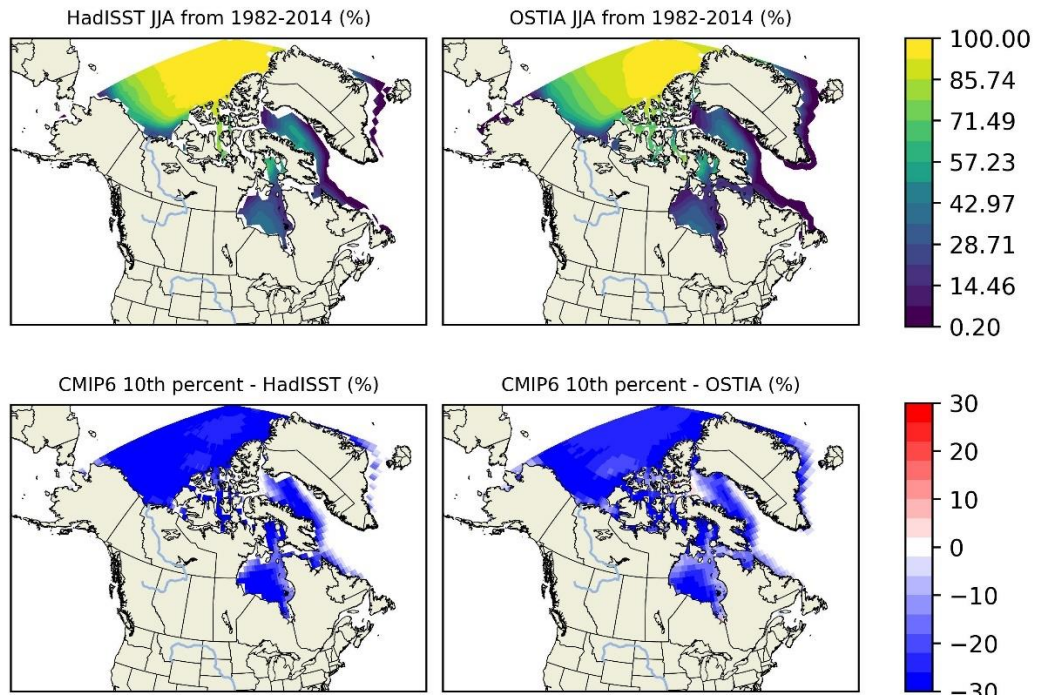
- SIC JJA and JJA bias of 50th Percentile (1982-2014)



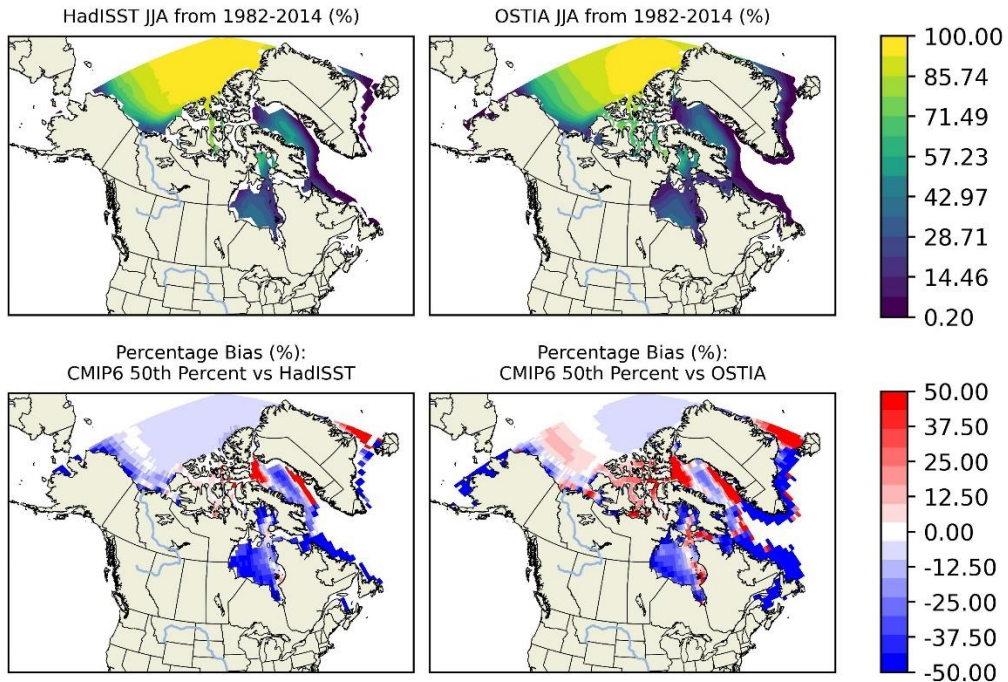
- SIC JJA and JJA bias of 90th Percentile (1982-2014)



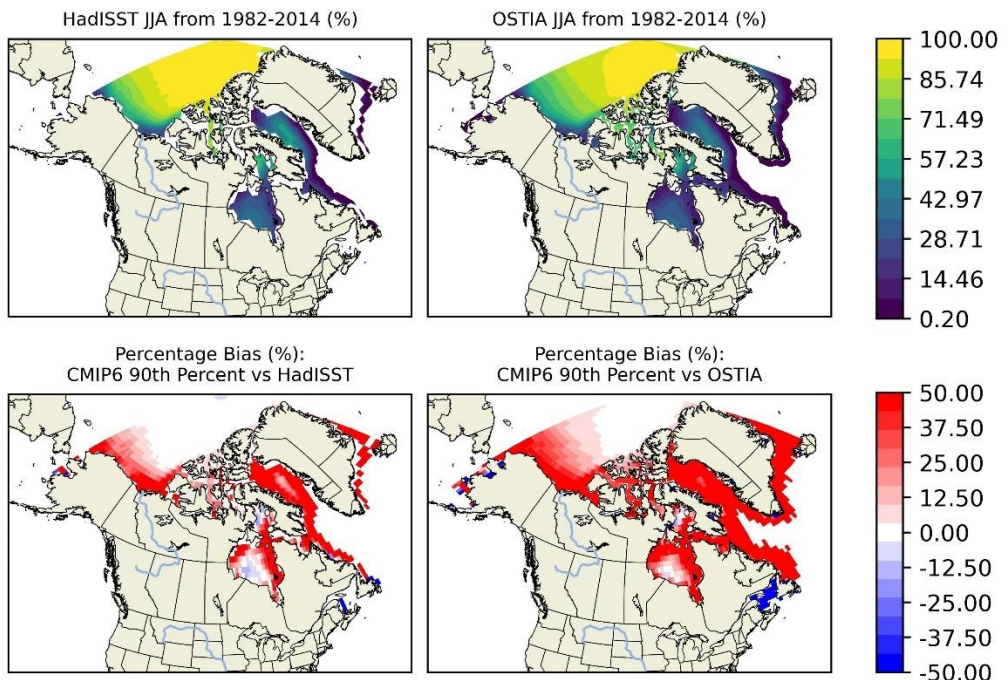
- SIC JJA and JJA bias of 10th Percentile (1982-2014)



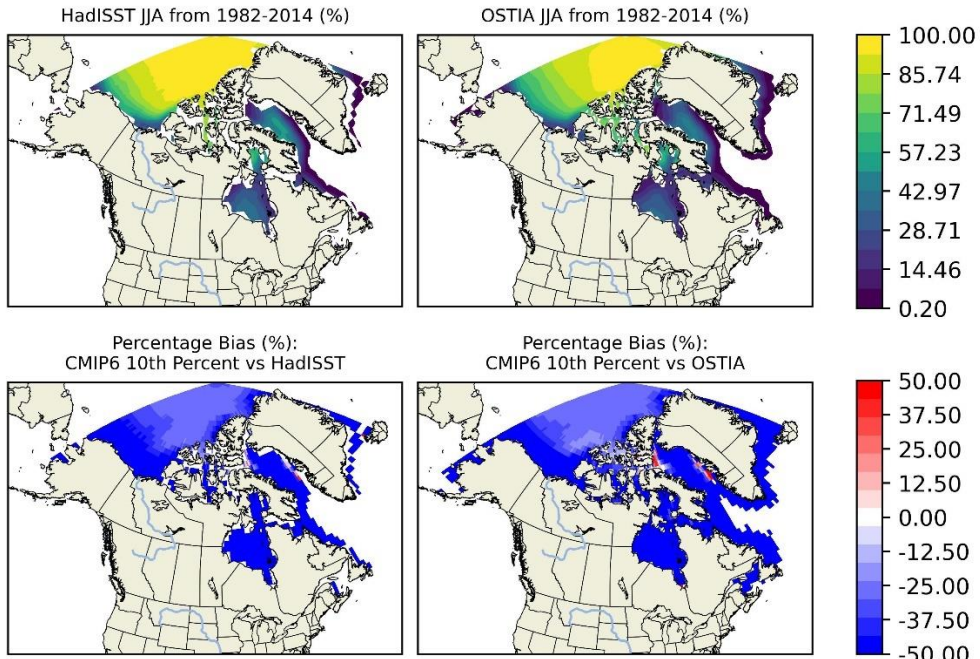
- SIC JJA and JJA percentage bias of 50th Percentile (1982-2014)



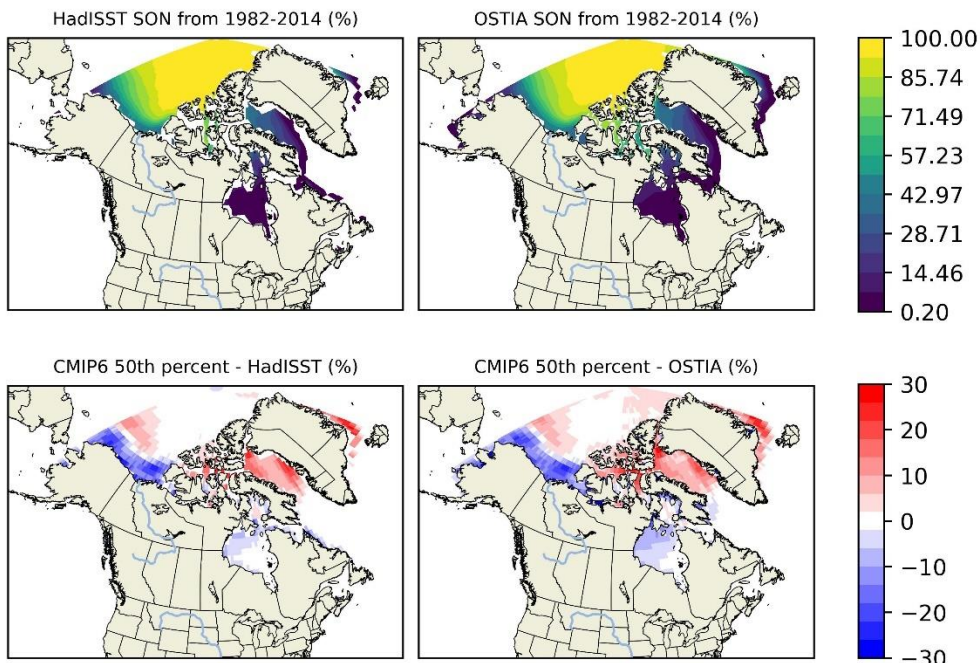
- SIC JJA and JJA percentage bias of 90th Percentile (1982-2014)



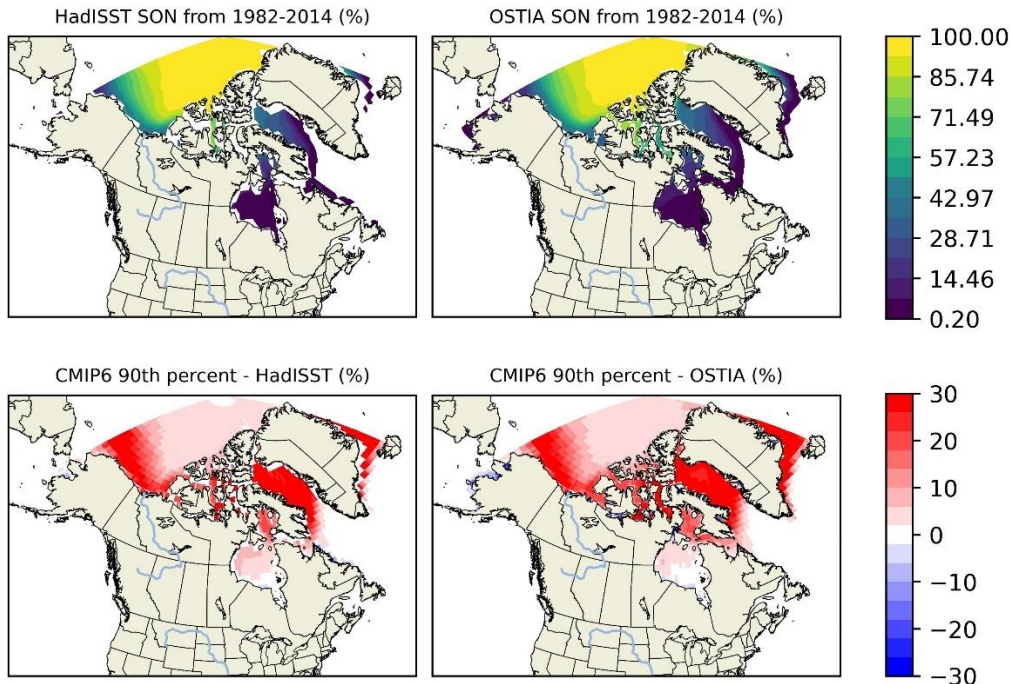
- SIC JJA and JJA percentage bias of 10th Percentile (1982-2014)



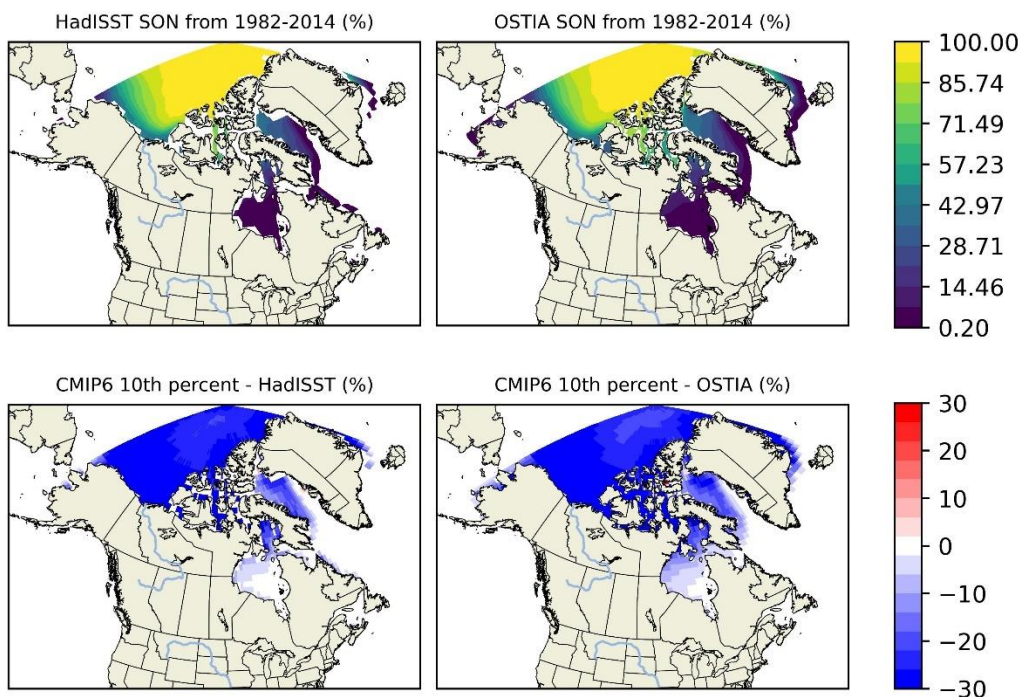
- SIC SON and SON bias of 50th Percentile (1982-2014)



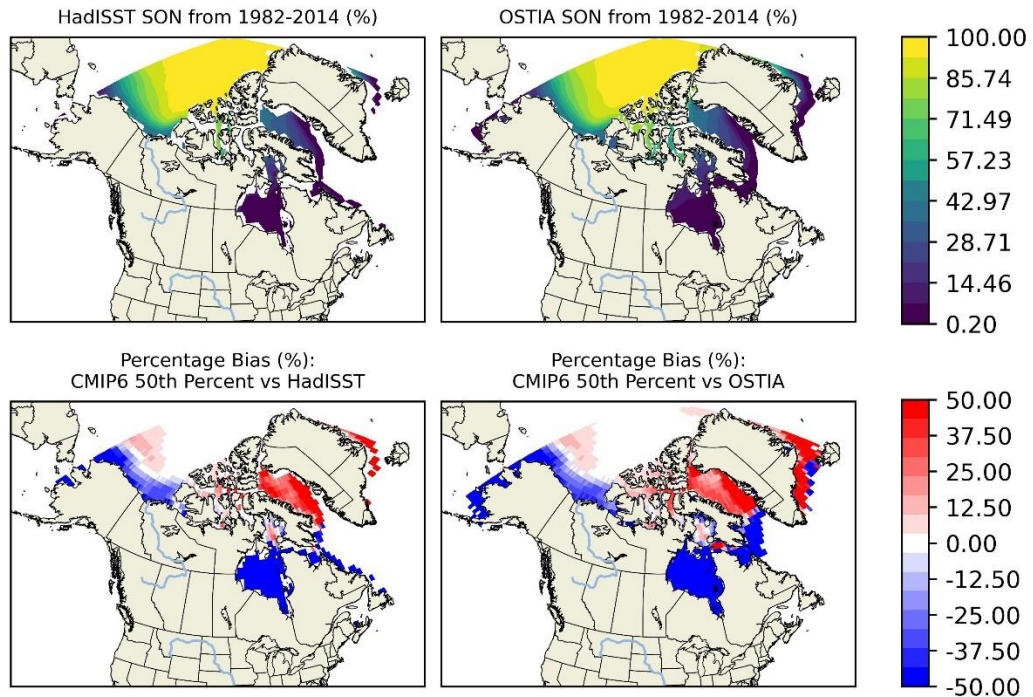
- SIC SON and SON bias of 90th Percentile (1982-2014)



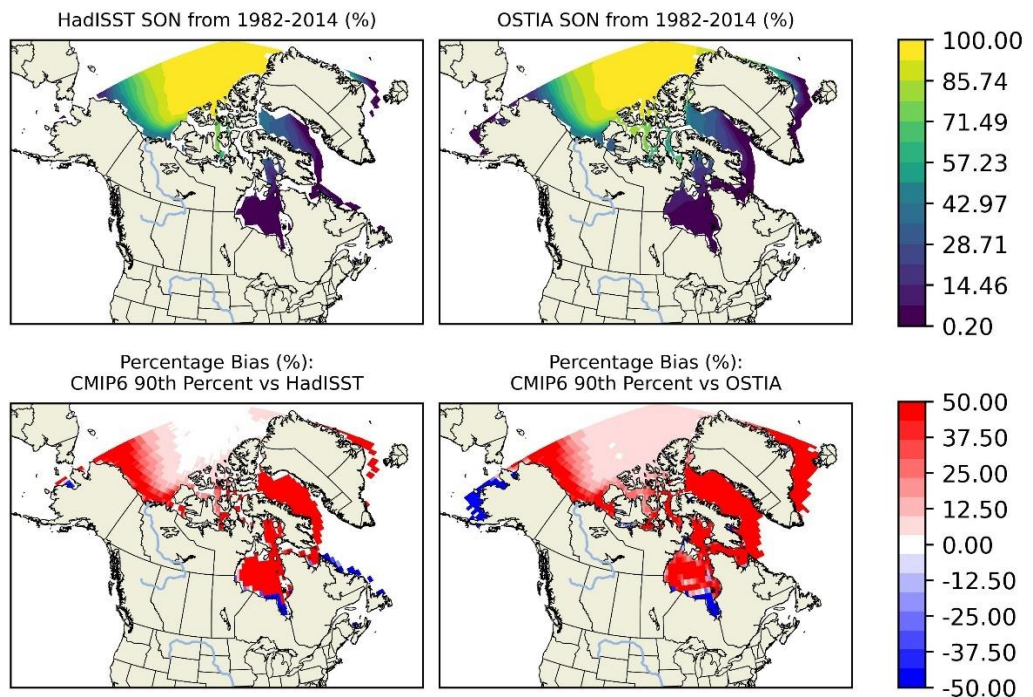
- SIC SON and SON bias of 10th Percentile (1982-2014)



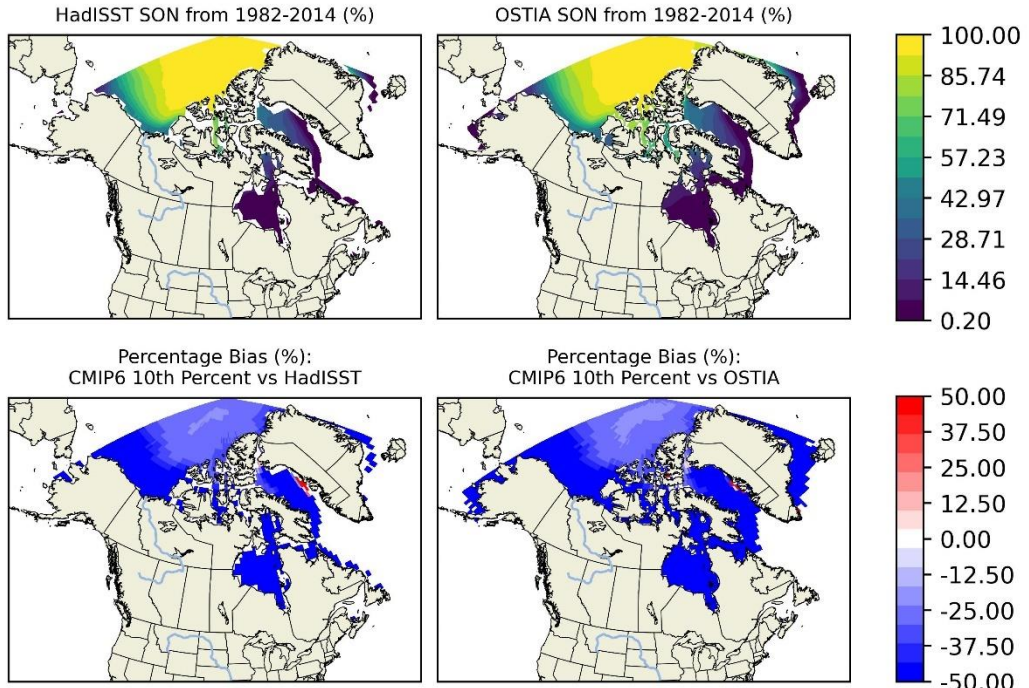
- SIC SON and SON percentage bias of 50th Percentile (1982-2014)



- SIC SON and SON percentage bias of 90th Percentile (1982-2014)

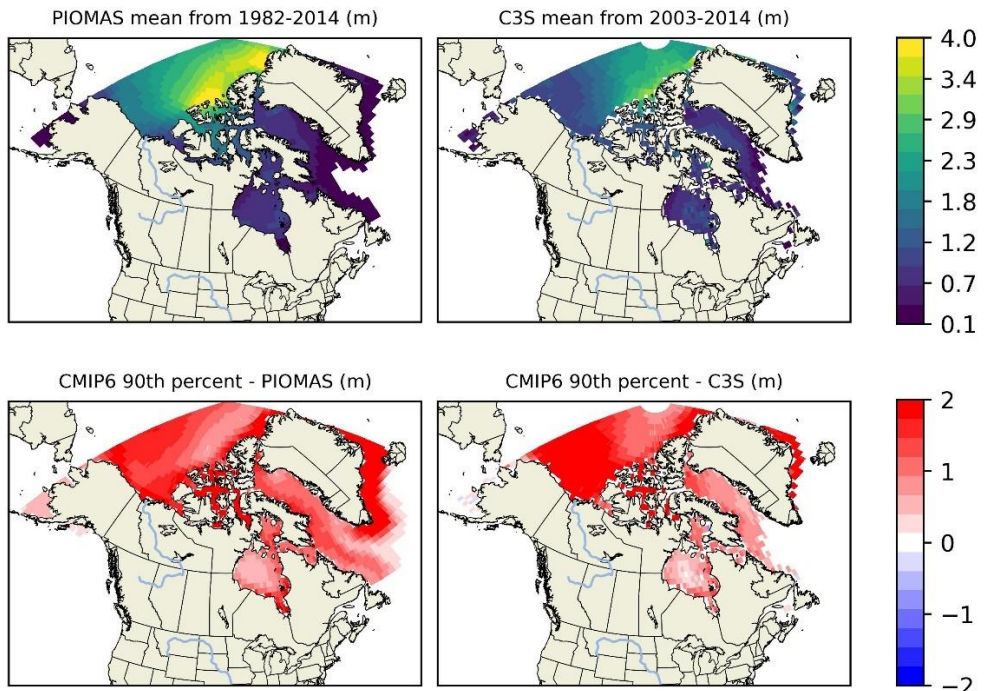


- SIC SON and SON percentage bias of 10th Percentile (1982-2014)

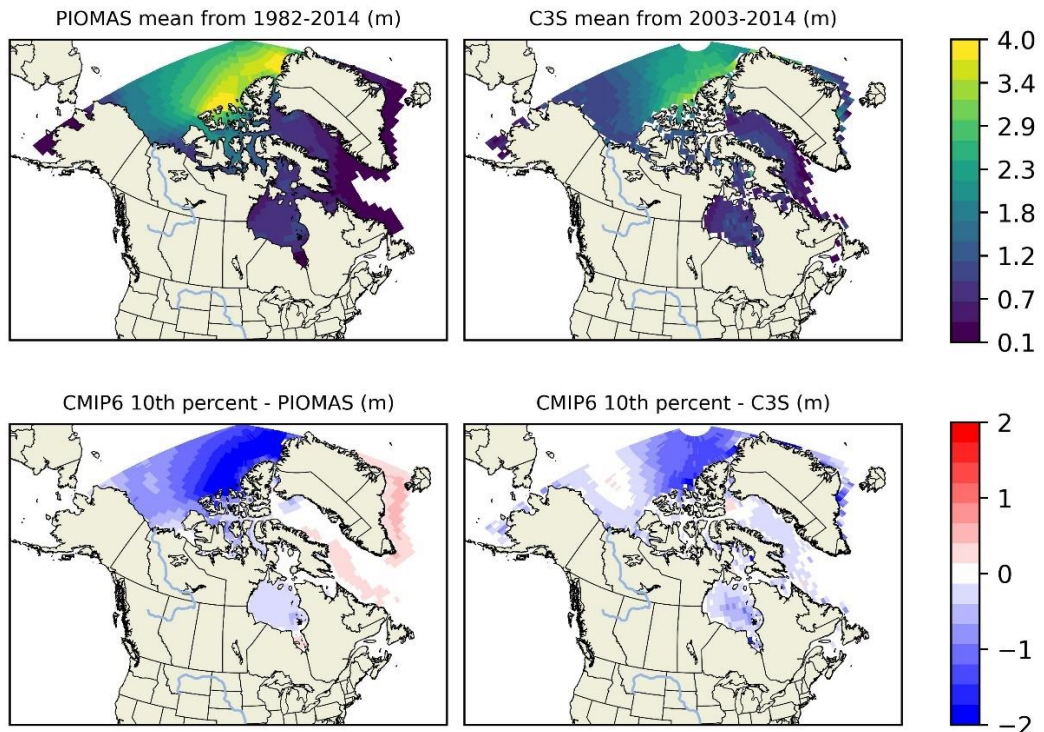


9.2 SIT

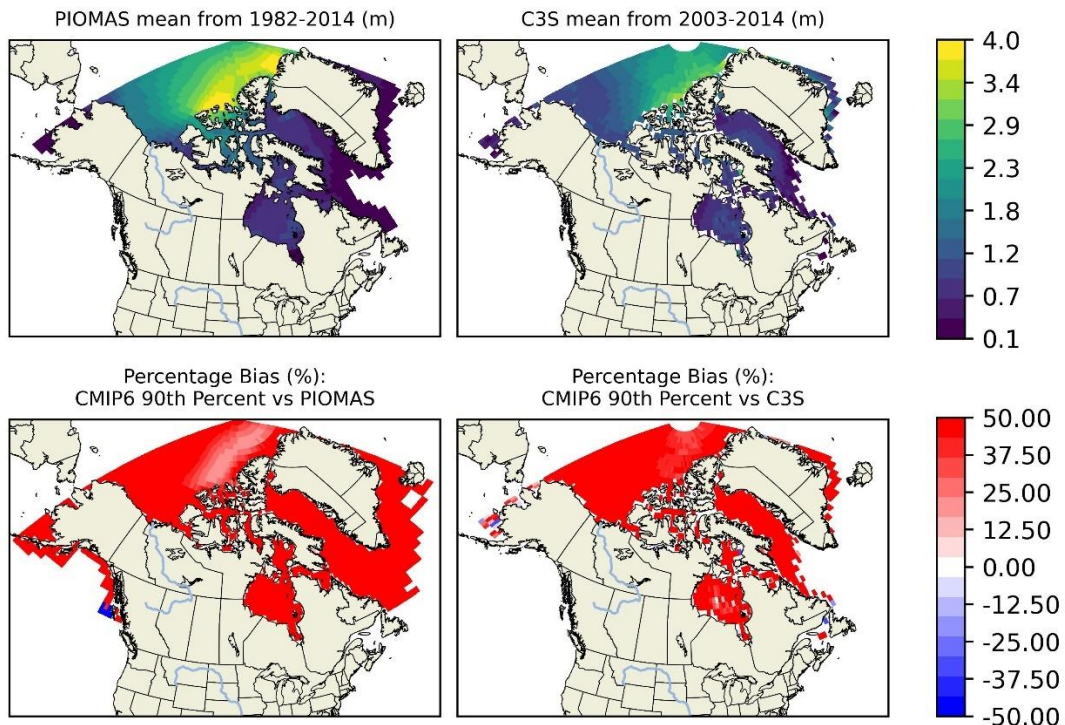
- SIT mean and mean bias of 90th Percentile (1982-2014: 2003-2014)



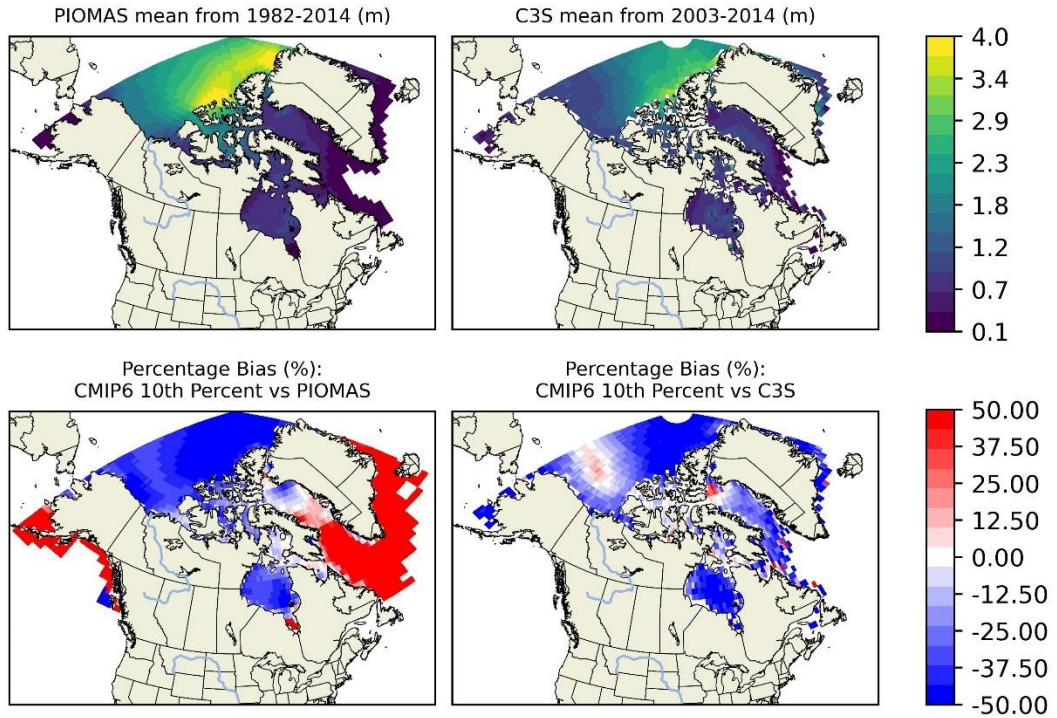
- SIT mean and mean bias of 10th Percentile (1982-2014: 2003-2014)



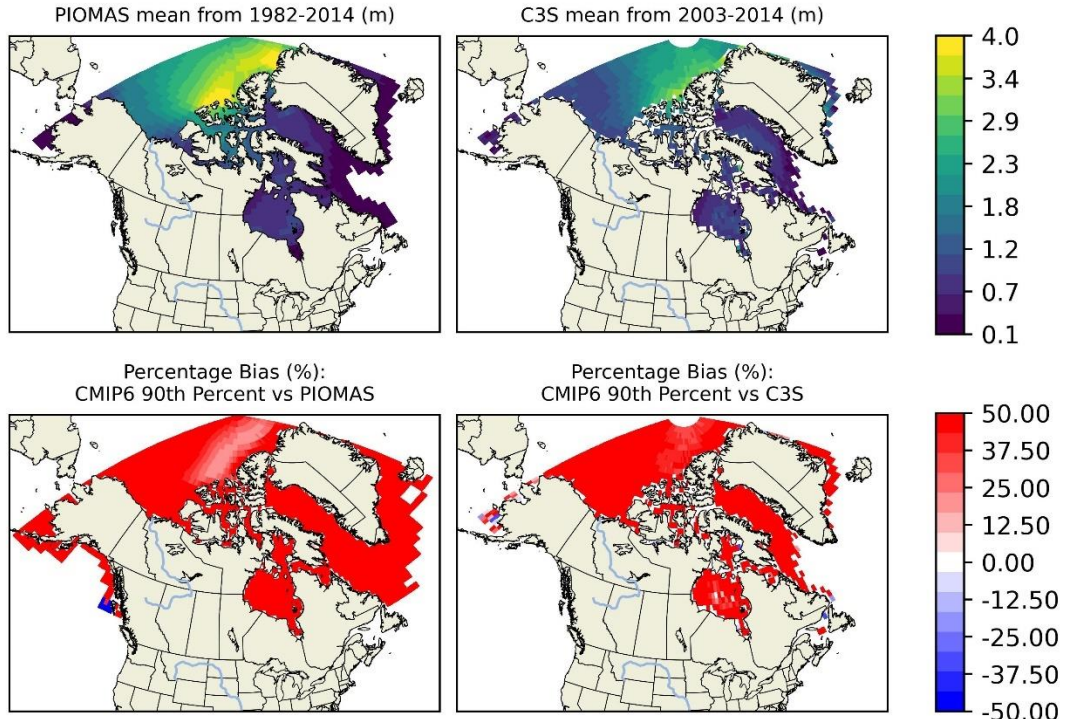
- SIT mean and percentage bias of 90th Percentile (1982-2014: 2003-2014)



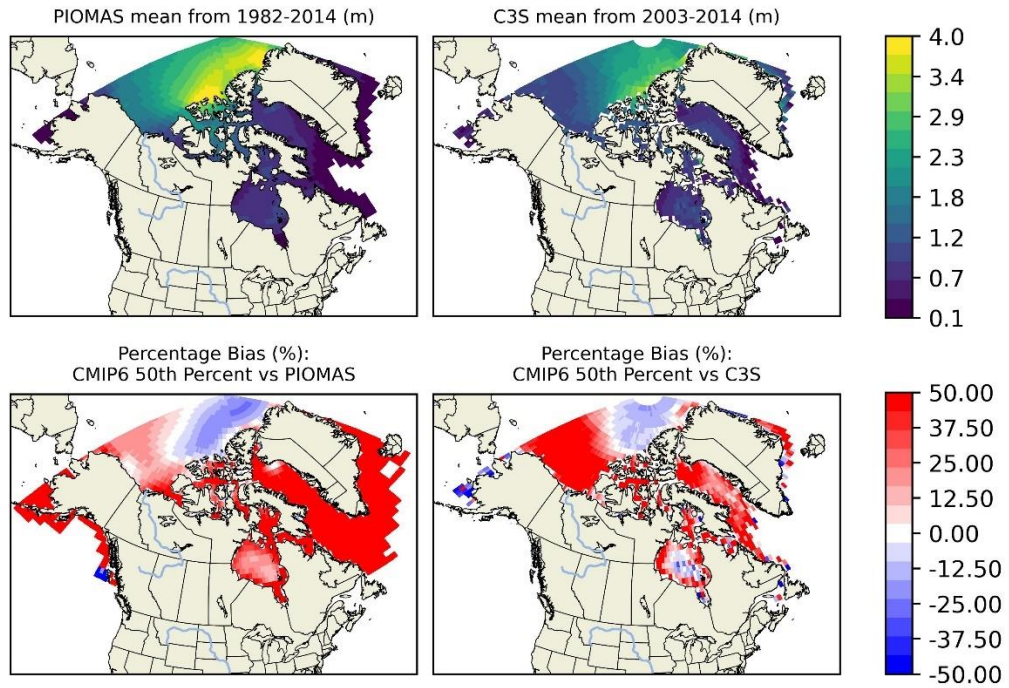
- SIT mean and percentage bias of 10th Percentile (1982-2014: 2003-2014)



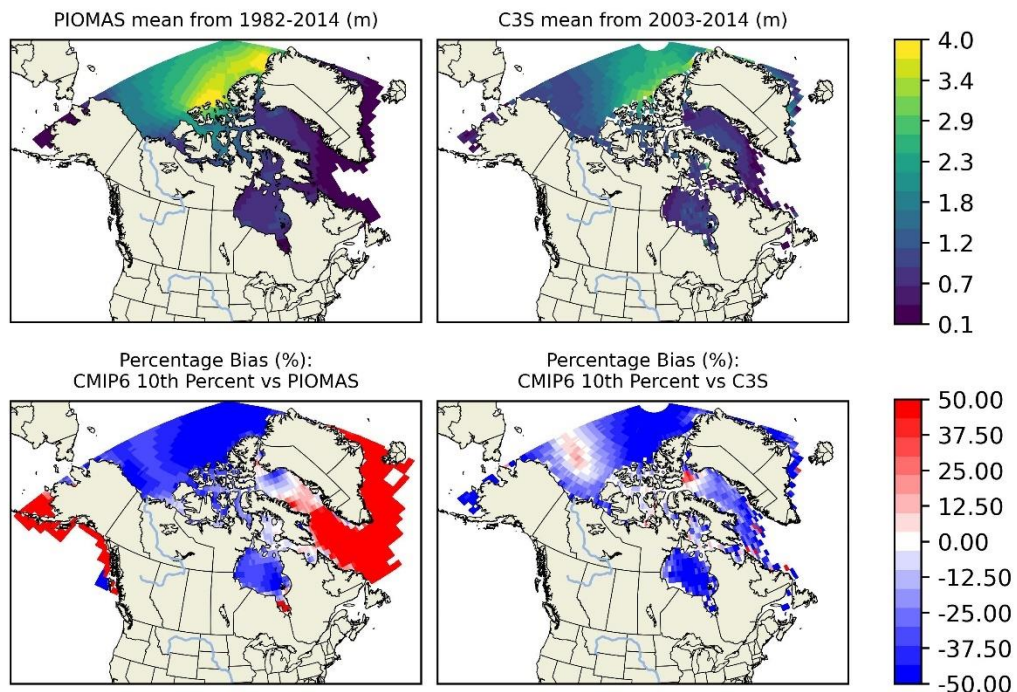
- SIT DJF and DJF percentage bias of 90th Percentile (1982-2014: 2003-2014)



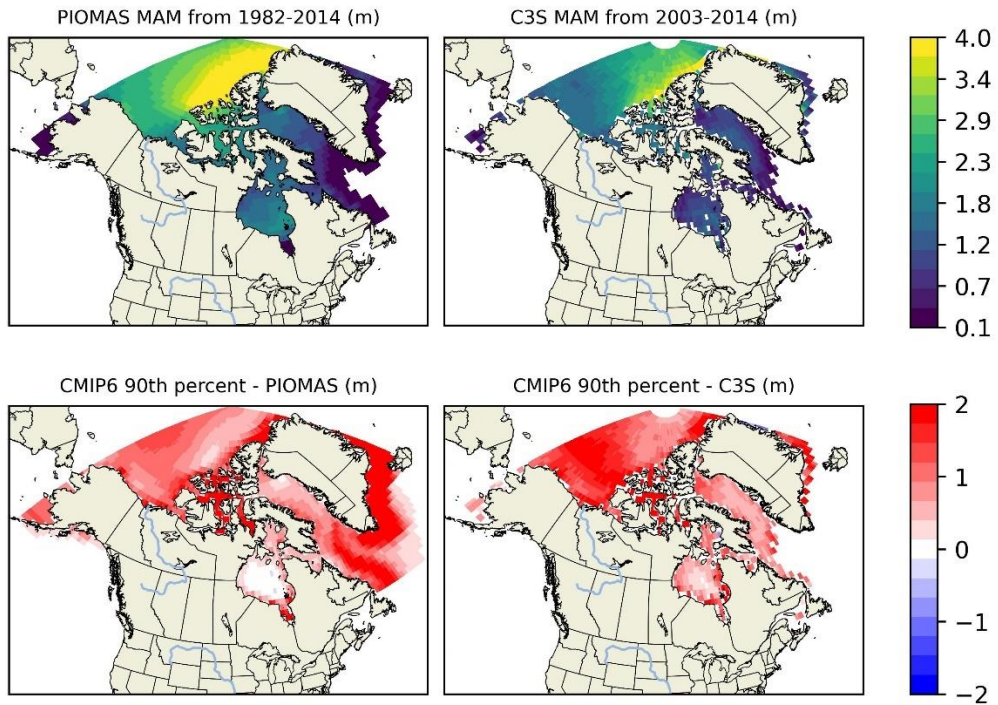
- SIT DJF and DJF percentage bias of 50th Percentile (1982-2014: 2003-2014)



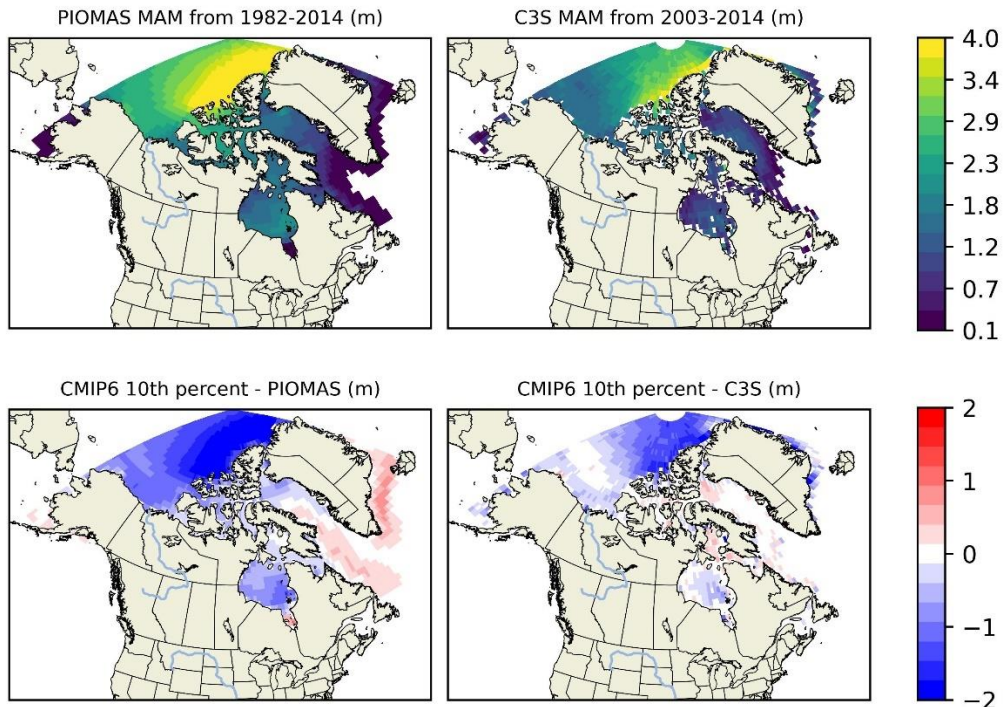
- SIT DJF and DJF percentage bias of 10th Percentile (1982-2014: 2003-2014)



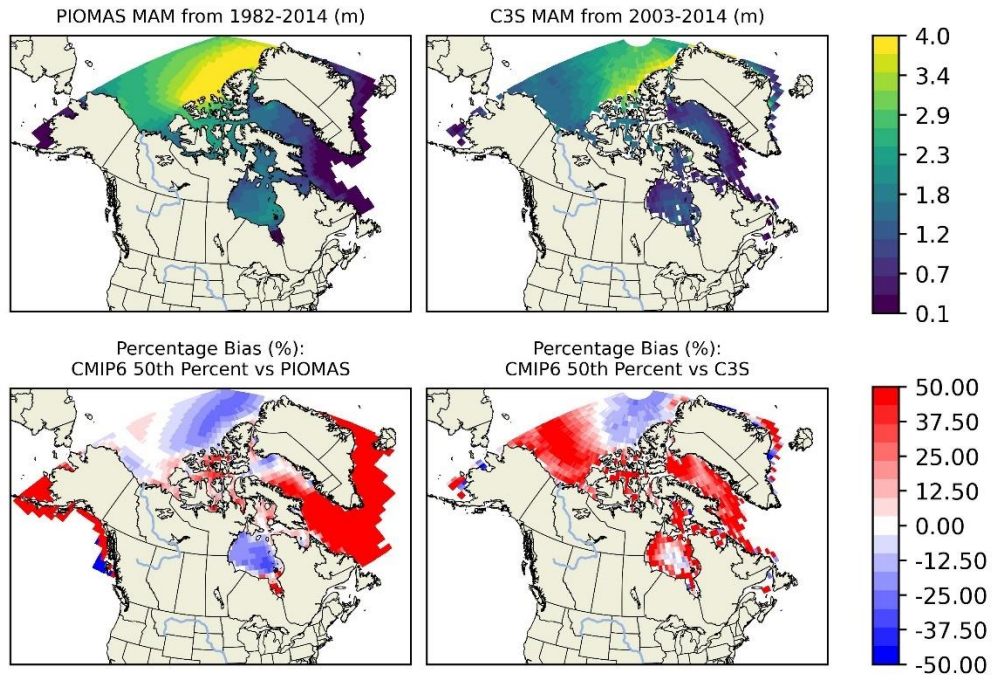
- SIT MAM and MAM bias of 90th Percentile (1982-2014: 2003-2014)



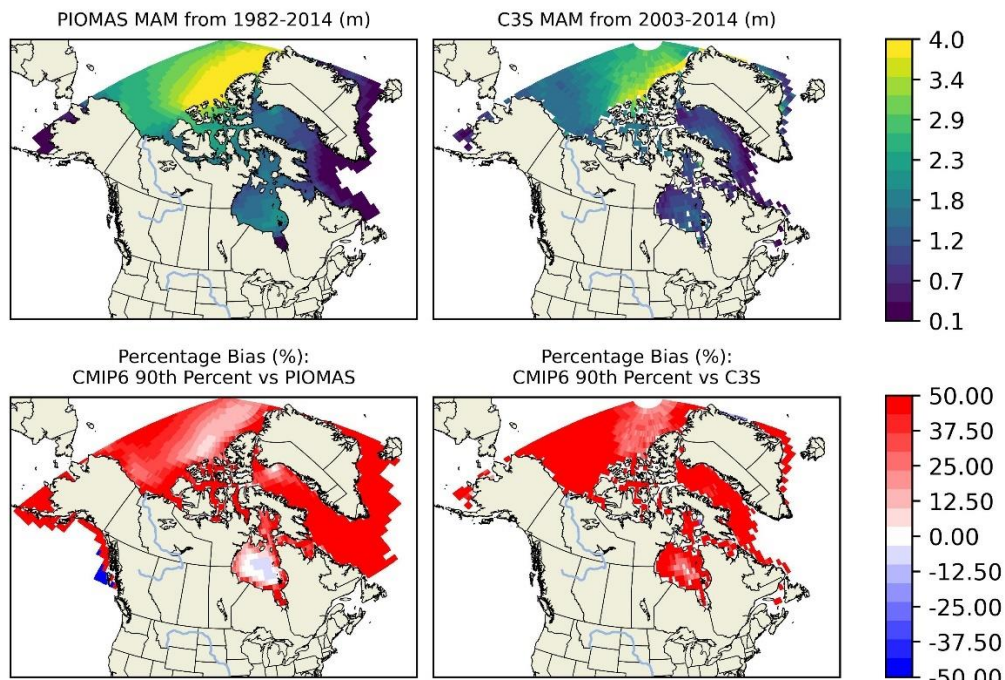
- SIT MA and MAM bias of 10th Percentile (1982-2014: 2003-2014)



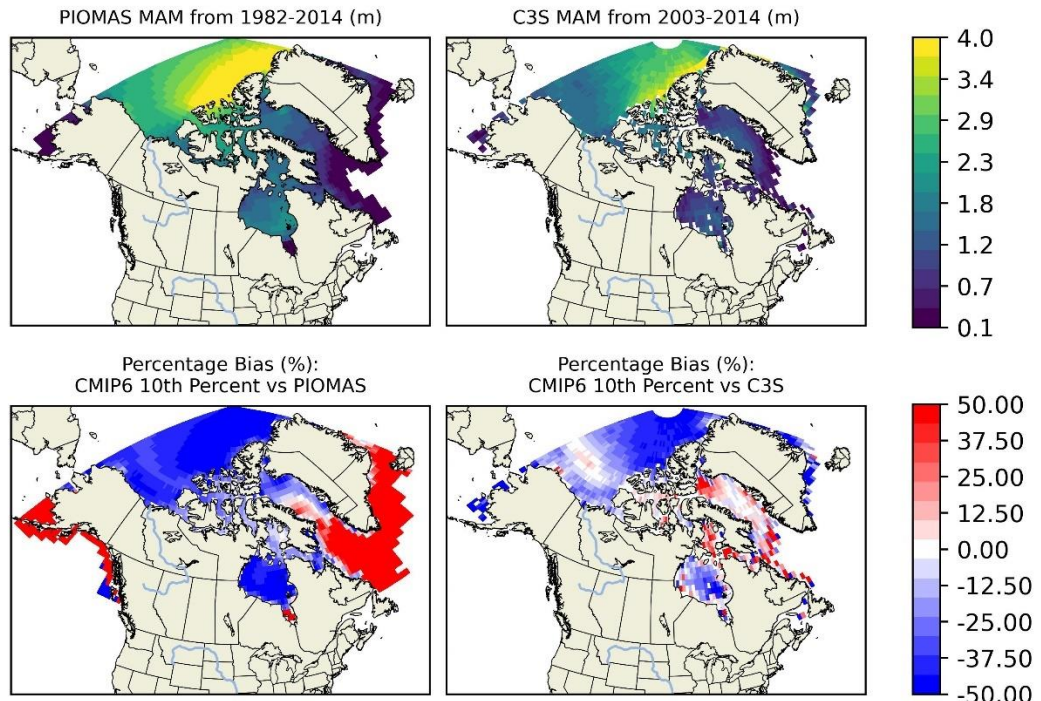
- SIT MAM and MAM percentage bias of 50th Percentile (1982-2014: 2003-2014)



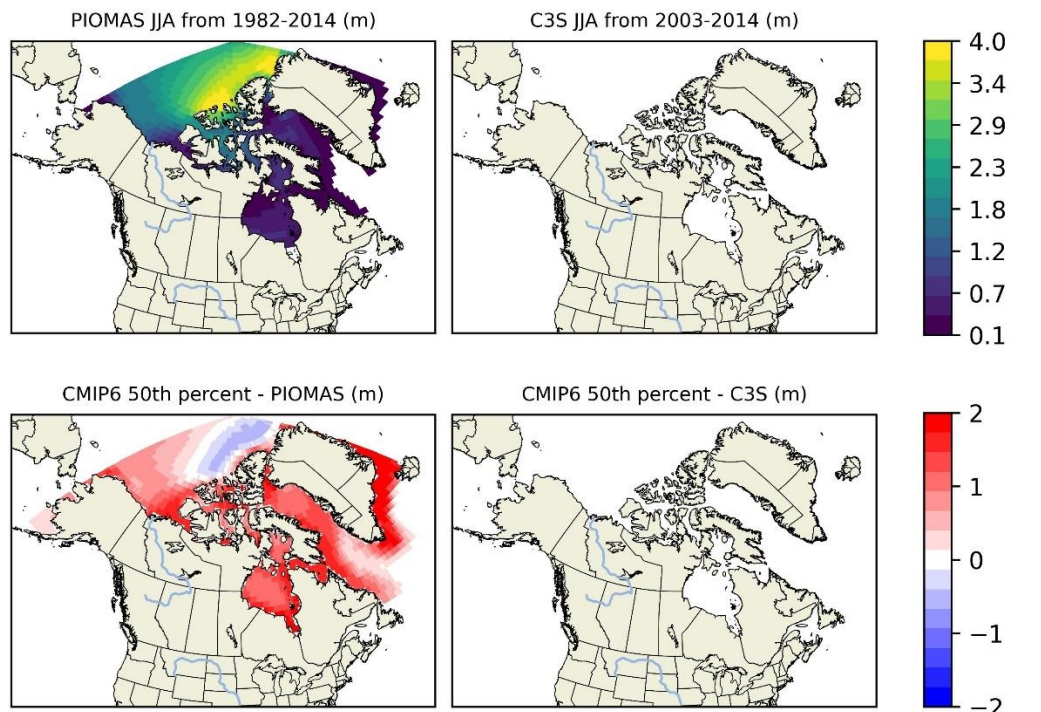
- SIT MAM and MAM percentage bias of 90th Percentile (1982-2014: 2003-2014)



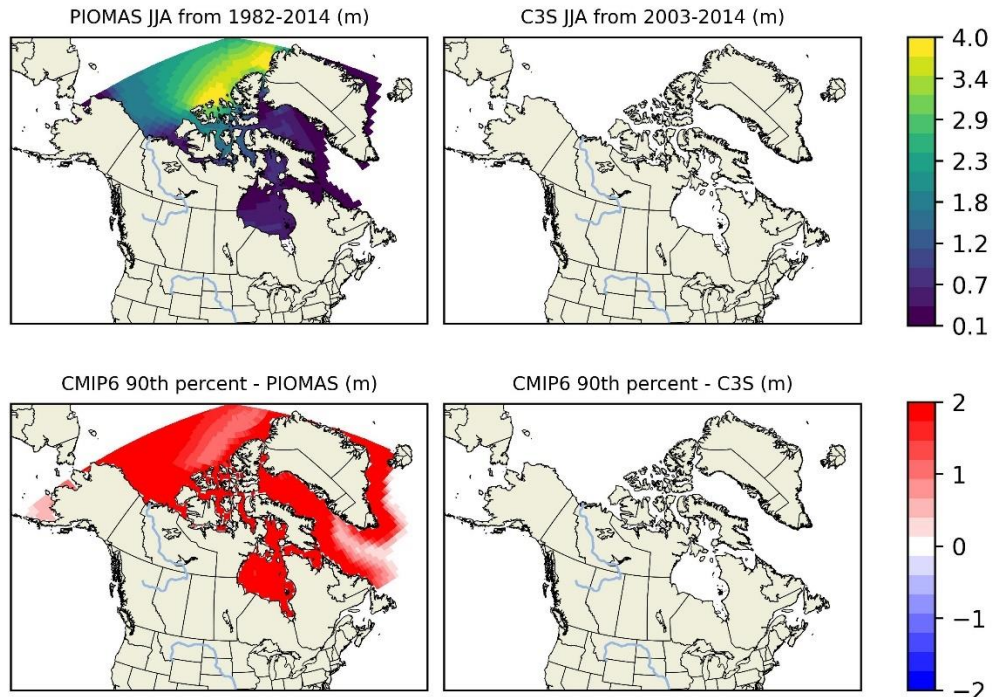
- SIT MAM and MAM percentage bias of 10th Percentile (1982-2014: 2003-2014)



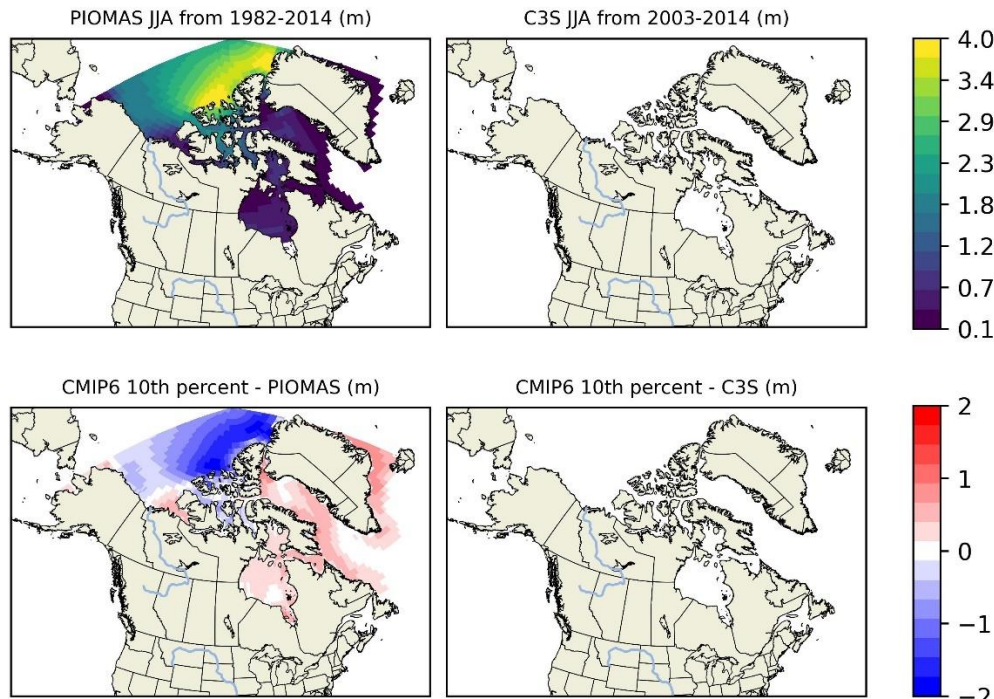
- SIT JJA and JJA bias of 50th Percentile (1982-2014: 2003-2014)



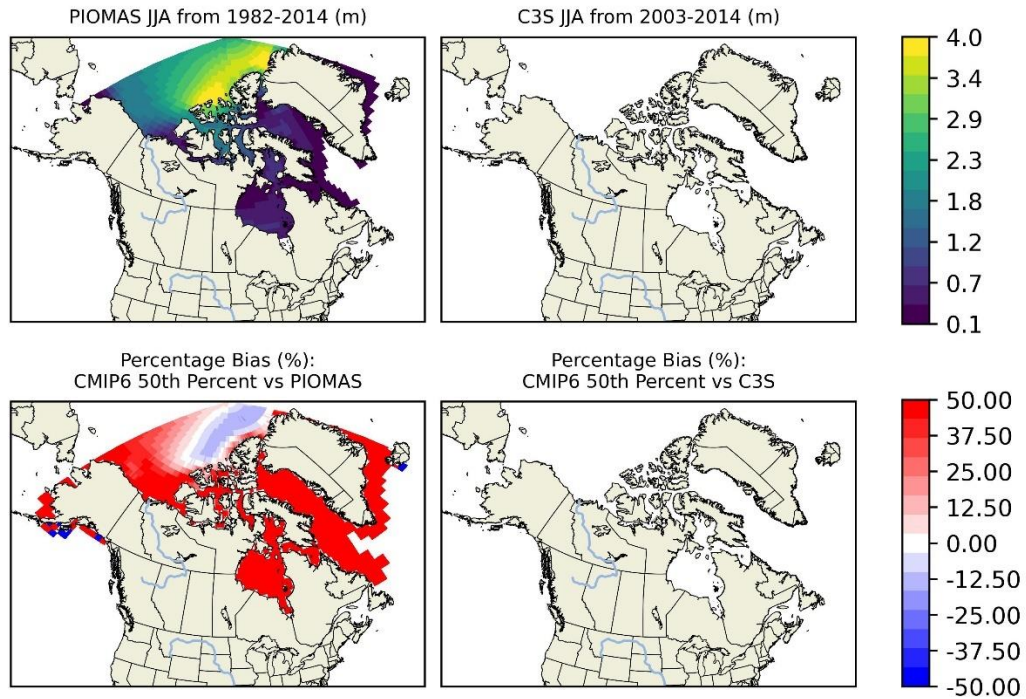
- SIT JJA and JJA bias of 90th Percentile (1982-2014: 2003-2014)



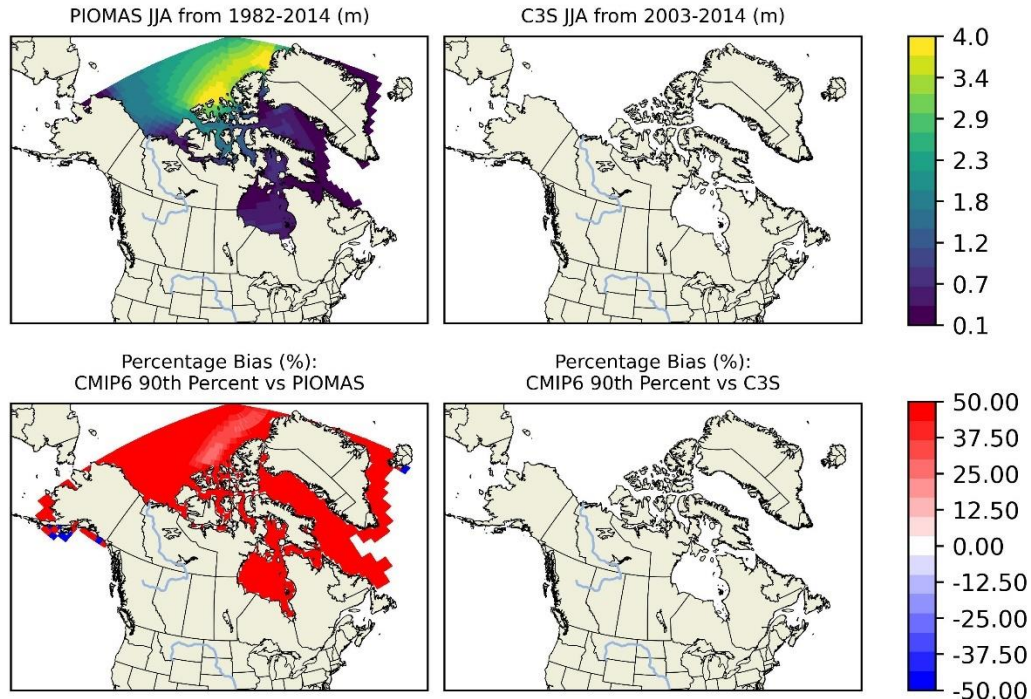
- SIT JJA and JJA bias of 10th Percentile (1982-2014: 2003-2014)



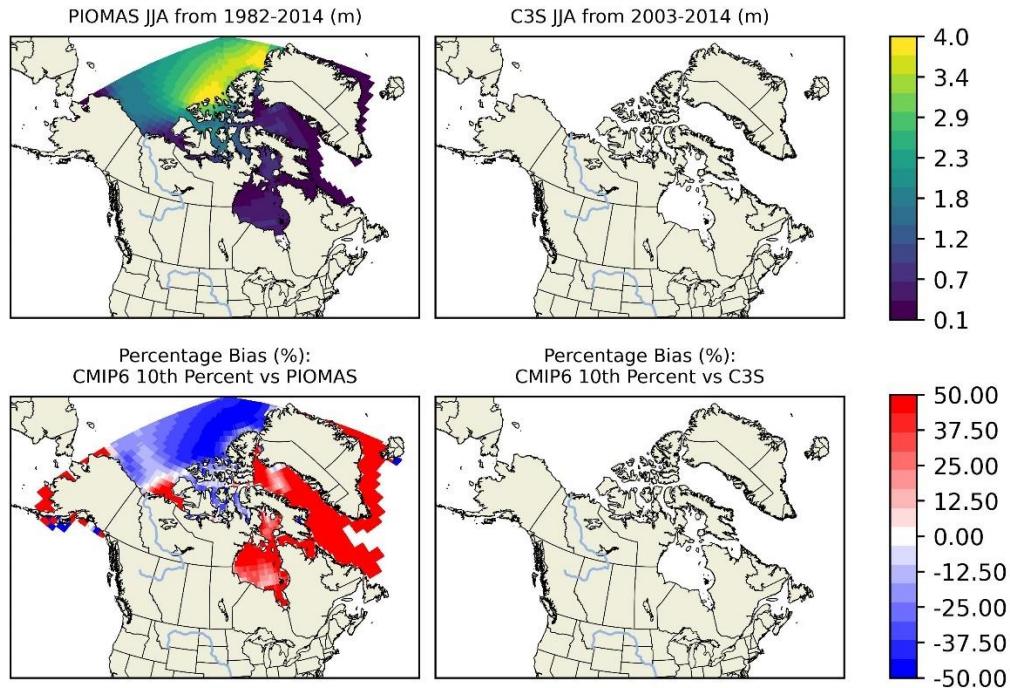
- SIT JJA and JJA percentage bias of 50th Percentile (1982-2014: 2003-2014)



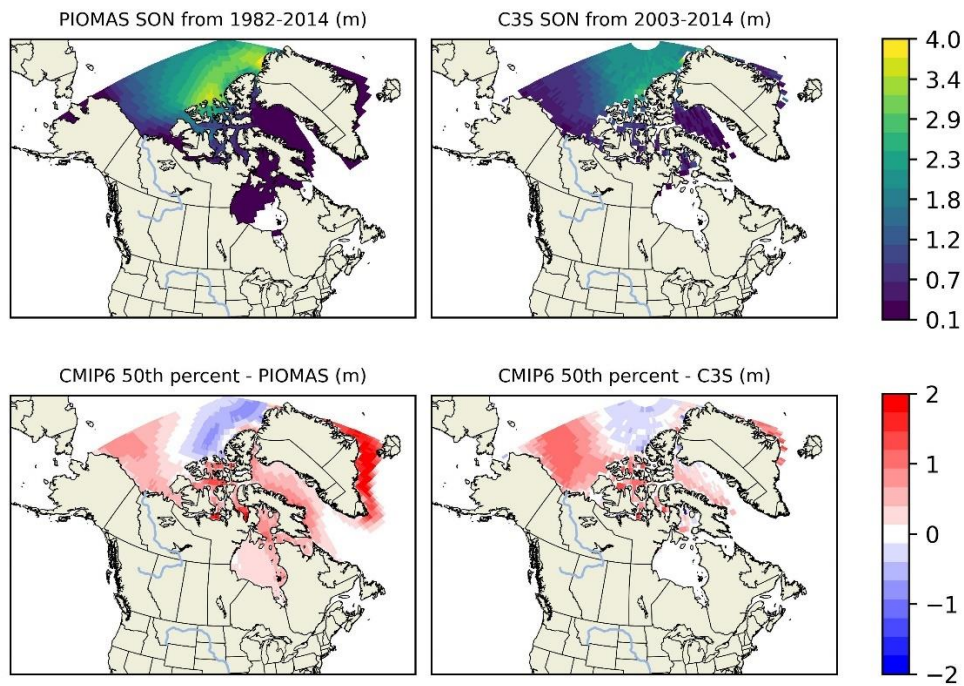
- SIT JJA and JJA percentage bias of 90th Percentile (1982-2014: 2003-2014)



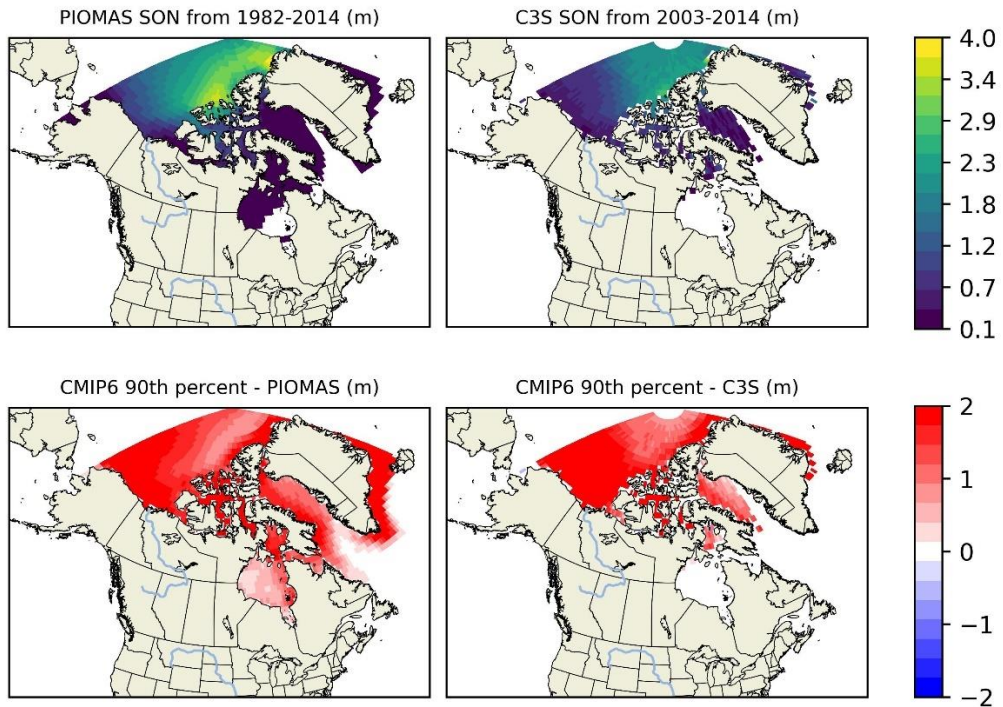
- SIT JJA and JJA percentage bias of 10th Percentile (1982-2014: 2003-2014)



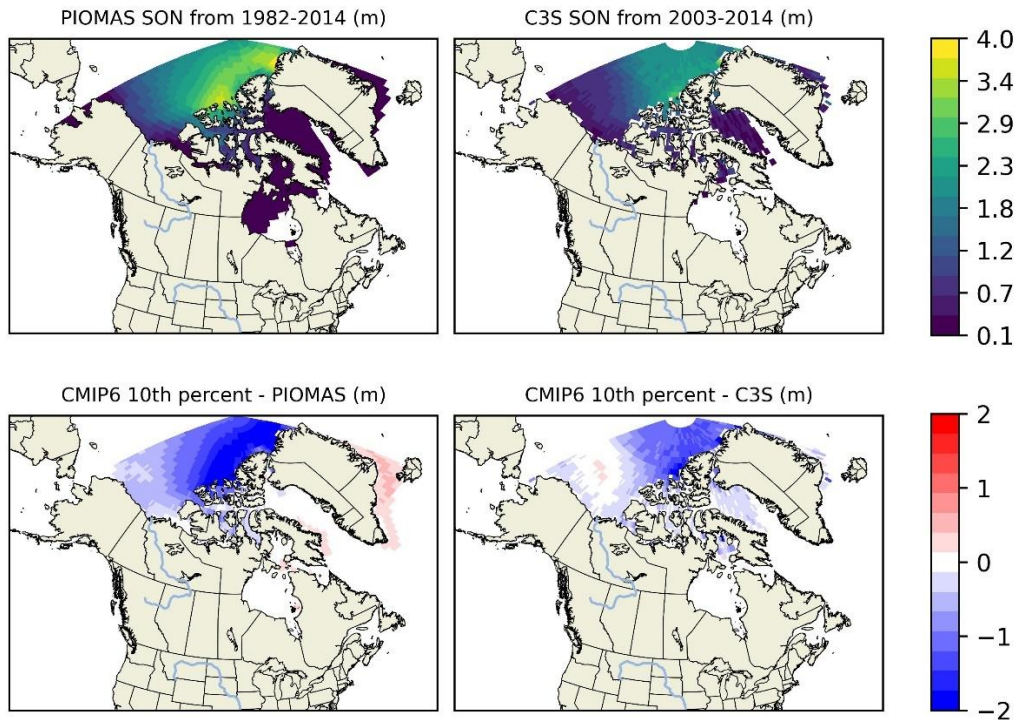
- SIT SON and SON bias of 50th Percentile (1982-2014: 2003-2014)



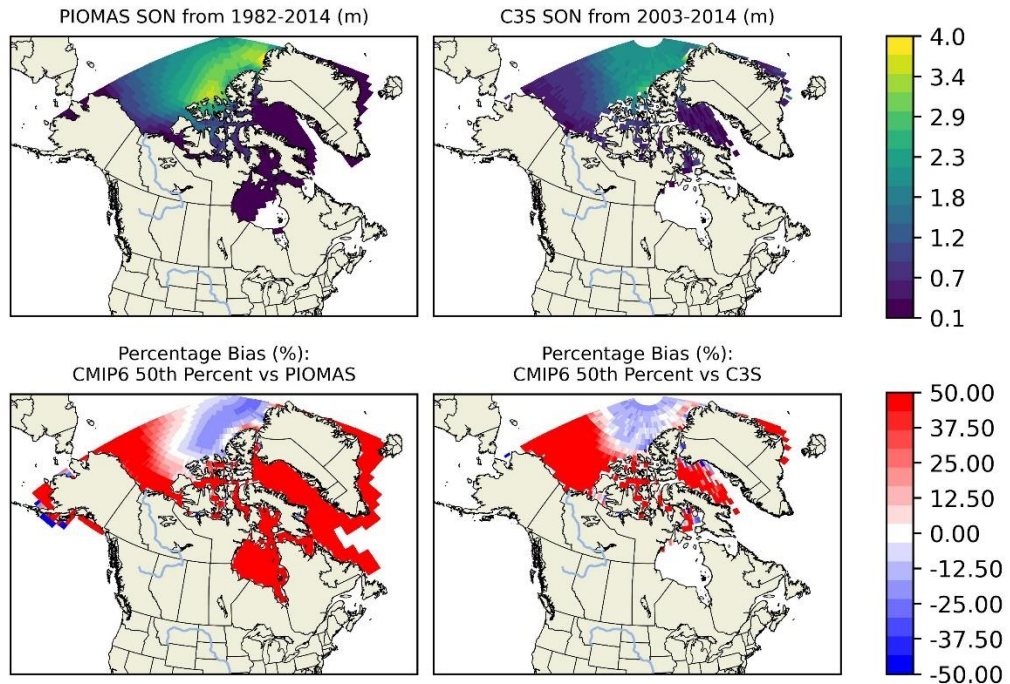
- SIT SON and SON bias of 90th Percentile (1982-2014: 2003-2014)



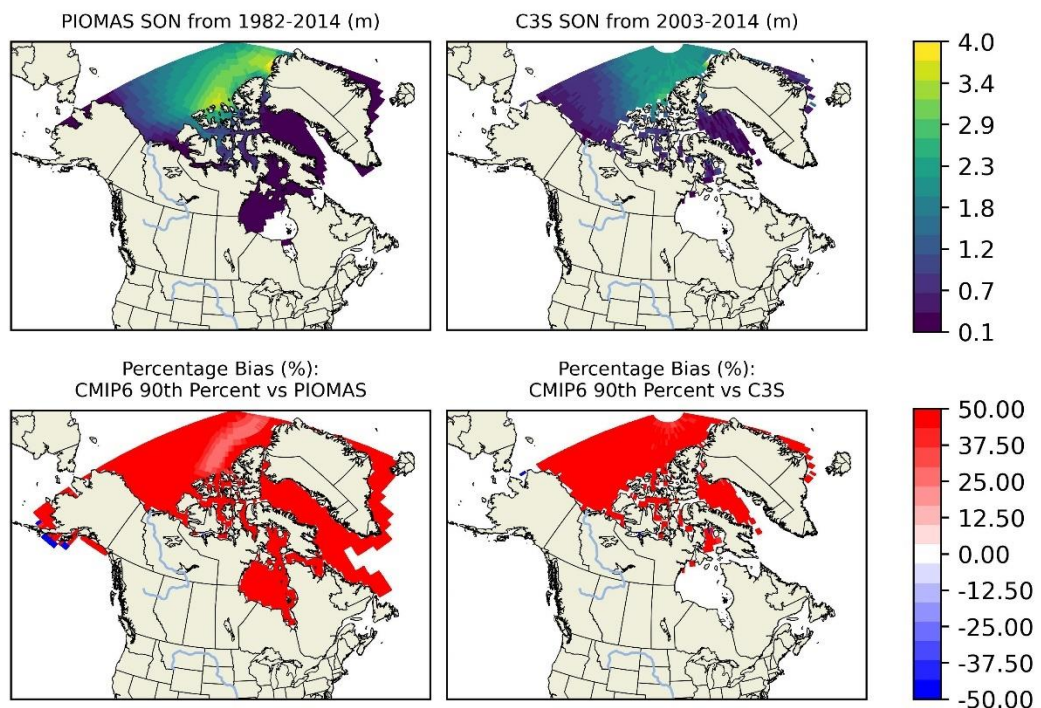
- SIT SON and SON bias of 10th Percentile (1982-2014: 2003-2014)



- SIT SON and SON percentage bias of 50th Percentile (1982-2014: 2003-2014)



- SIT SON and SON percentage bias of 90th Percentile (1982-2014: 2003-2014)



- SIT SON and SON percentage bias of 10th Percentile (1982-2014: 2003-2014)

